European Research Council
Established by the European Commission

Deutsche Forschungsgemeinschaft

www.computational-relativity.org

Modeling the strong-field dynamics of binary neutron star mergers

S.Bernuzzi

FRIEDRICH-SCHILLER-UNIVERSITÄT JENA

NEB 21. - Corfu - Sept 2025

Binary neutron star mergers: cosmic labs for fundamental and astro physics

Strong-gravity probe
GW evidence (Hulse&Taylor)

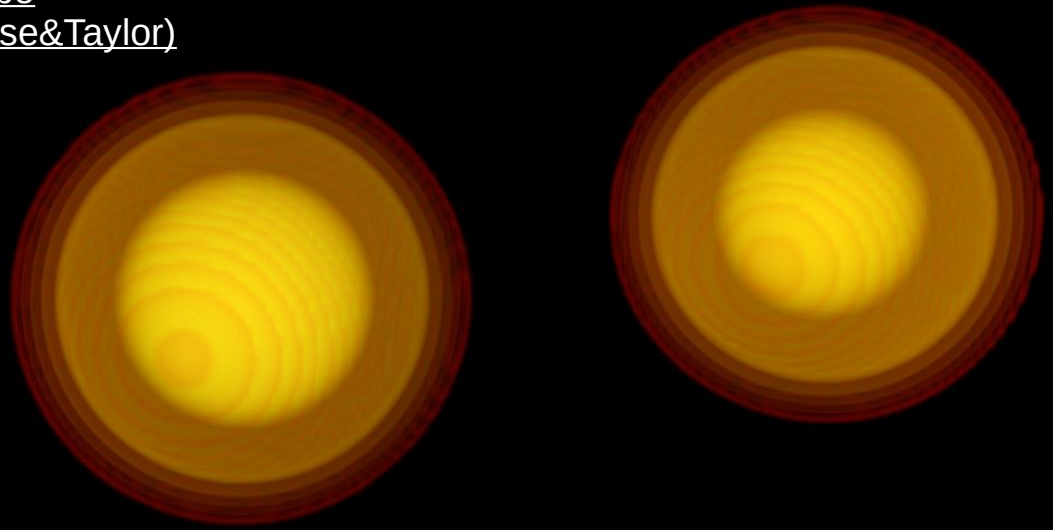

Extreme matter densities
Constraints on equation of state (EOS)

Binary neutron star mergers: cosmic labs for fundamental and astro physics

Strong-gravity probe
GW evidence (Hulse&Taylor)

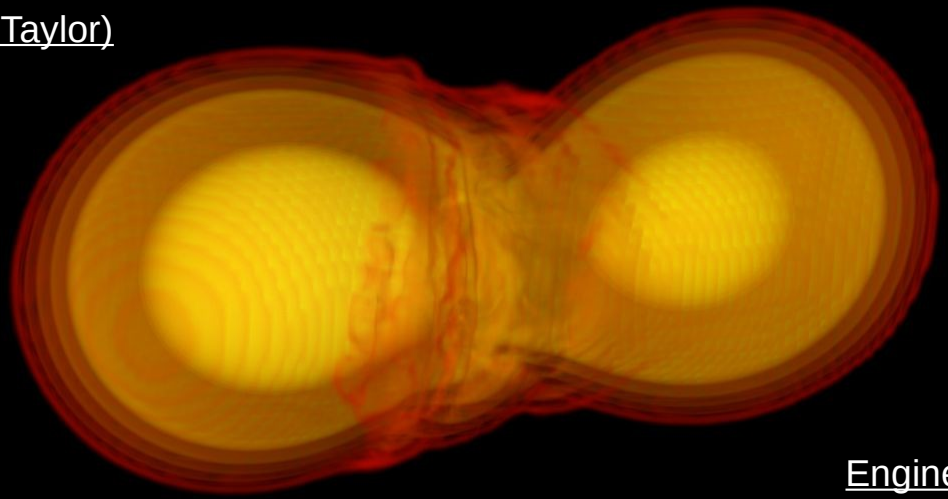

Engines for high-energy EM emissions
Gamma-ray / kilonova transients

Extreme matter densities
Constraints on equation of state (EOS)

Standard Sirens
Cosmolography & Hubble tension

Binary neutron star mergers: cosmic labs for fundamental and astro physics

Strong-gravity probe
GW evidence (Hulse&Taylor)

Neutron-rich outflows
Heavy elements nucleosynthesis

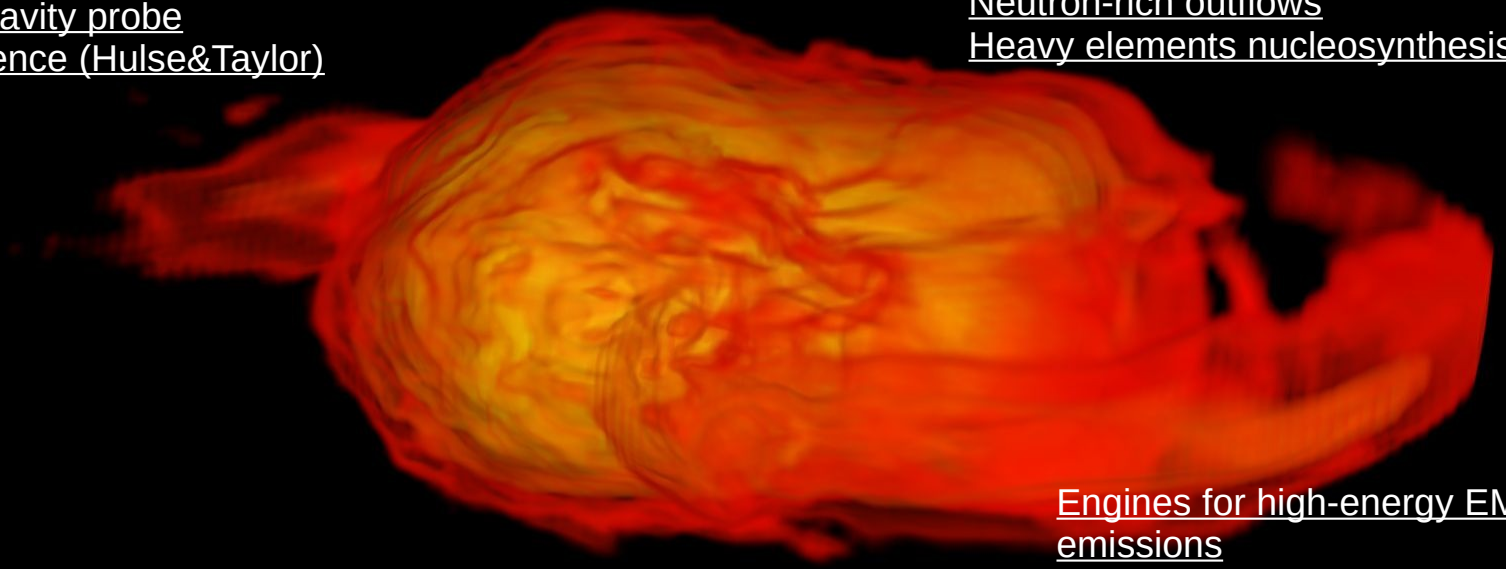

Engines for high-energy EM emissions
Gamma-ray / kilonova transients

Extreme matter densities
Constraints on equation of state (EOS)

Standard Sirens
Cosmolography & Hubble tension

First-principles models for observations

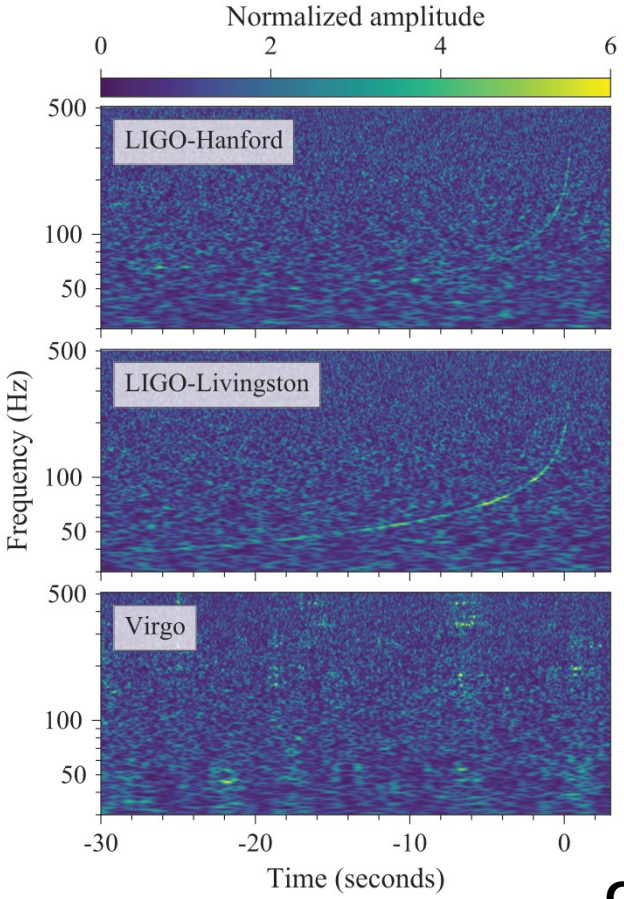

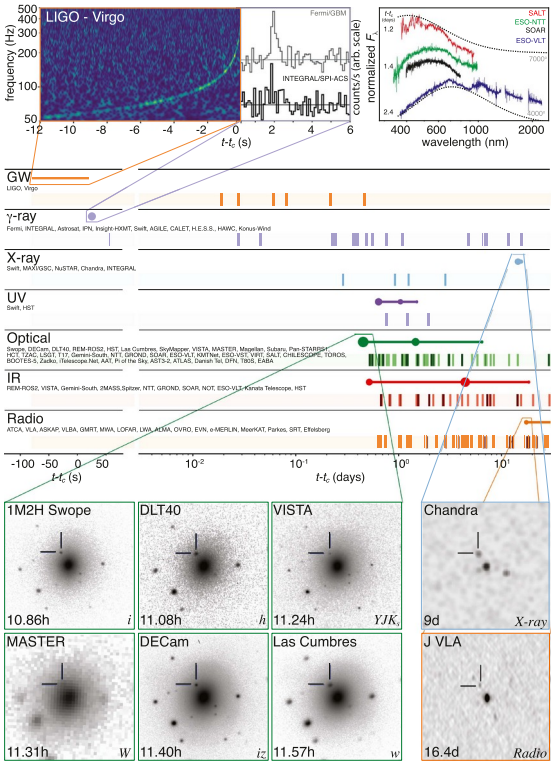

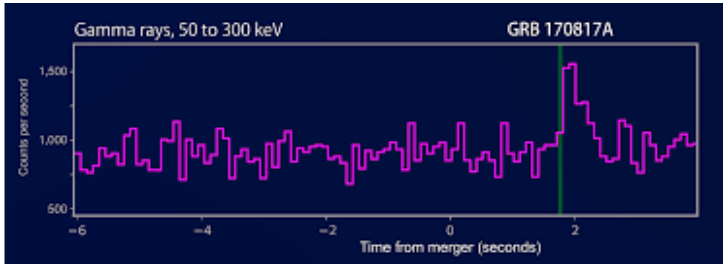

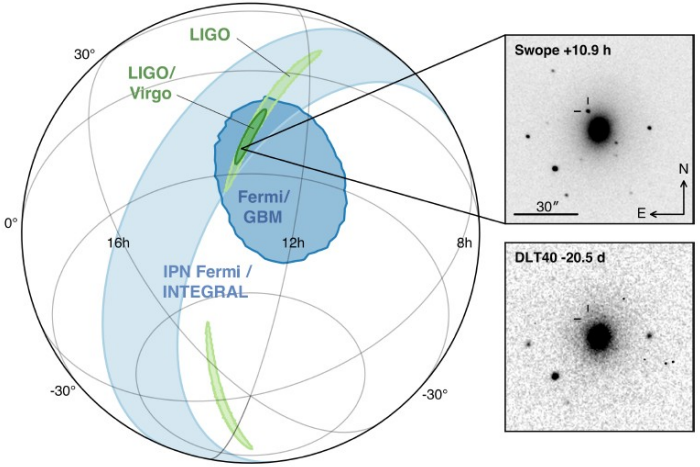

GW170817 August, 17th 2017, 12:41:01 UTC

Constraints on EOS after GW170817

NS radius GW170817+AT2017gfo
$R_{1.4} = 12.2^{+0.5}_{-0.5}$km

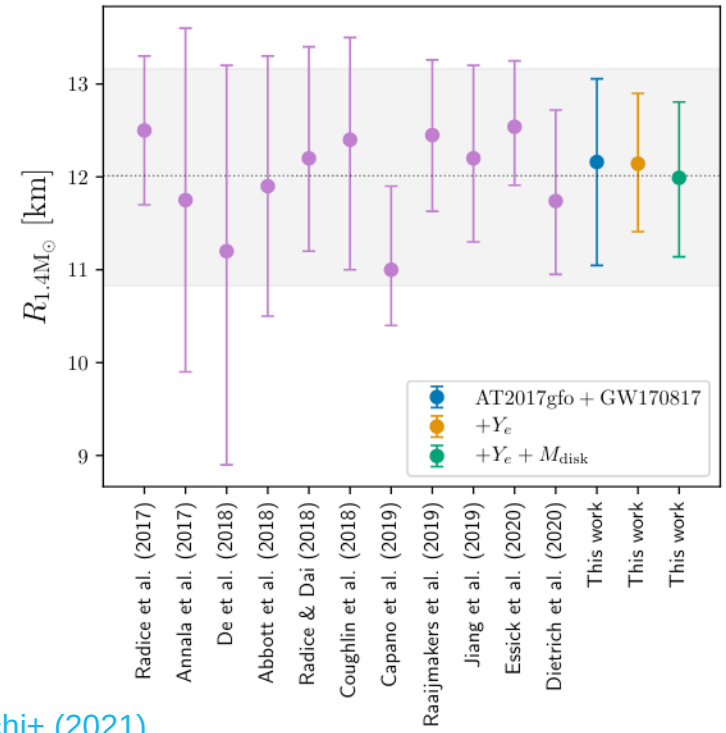

Breschi+ (2021)

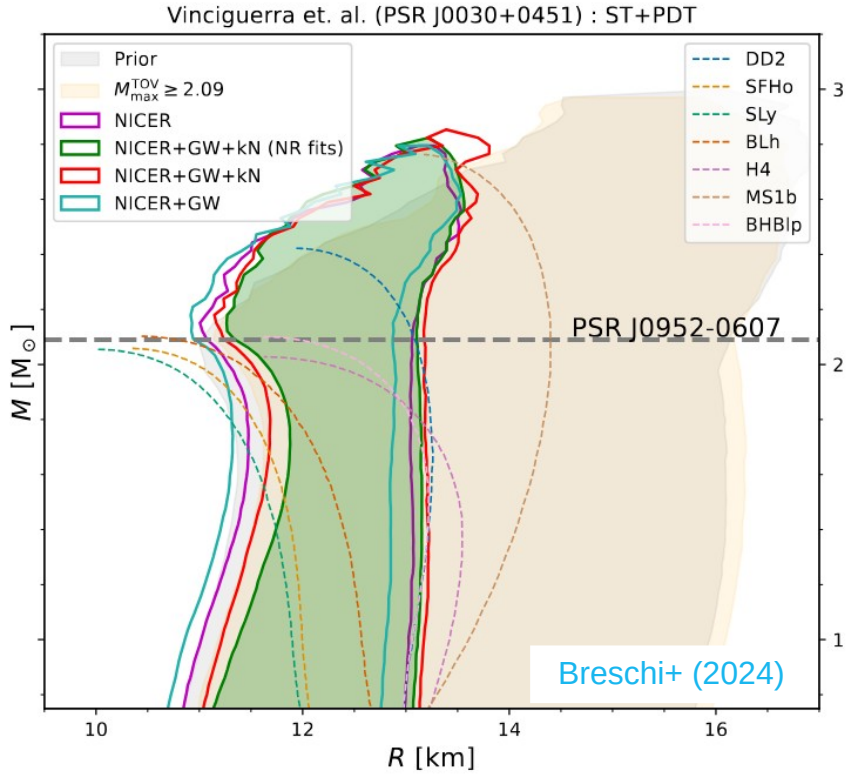

Mass-radius diagram from joint & coherent inference
+ PSR J0952–0607, J0030+0451, 0740+6620

Constraints on EOS after GW170817

NS radius GW170817+AT2017gfo
$R_{1.4} = 12.2^{+0.5}_{-0.5}$km

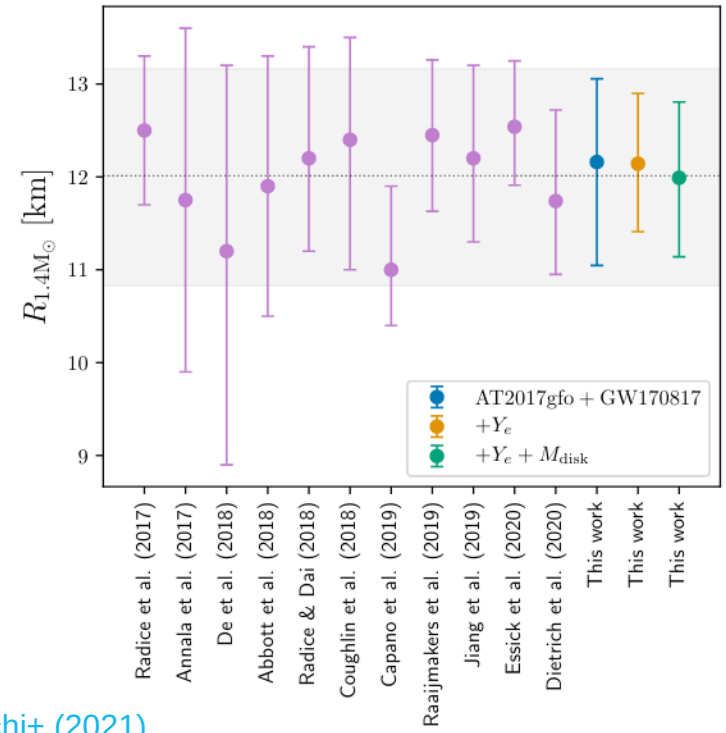

Breschi+ (2021)

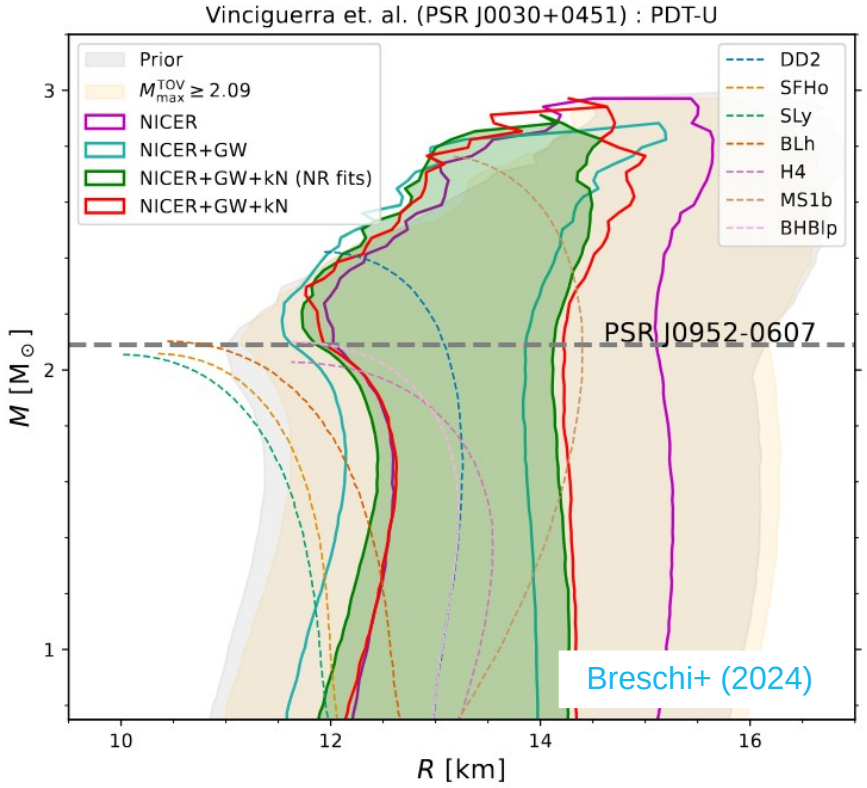

Breschi+ (2024)

Mass-radius diagram from joint & coherent inference
+ PSR J0952–0607, J0030+0451, 0740+6620

The complete GW spectrum

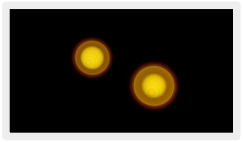

SB+ [https://arxiv.org/abs/1504.01764]
Breschi,SB+ [https://arxiv.org/abs/1908.11418]
Breschi,SB+ [https://arxiv.org/abs/2205.09112]

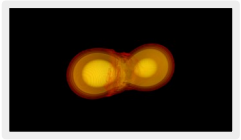

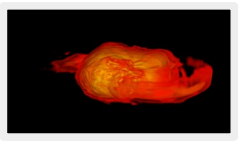

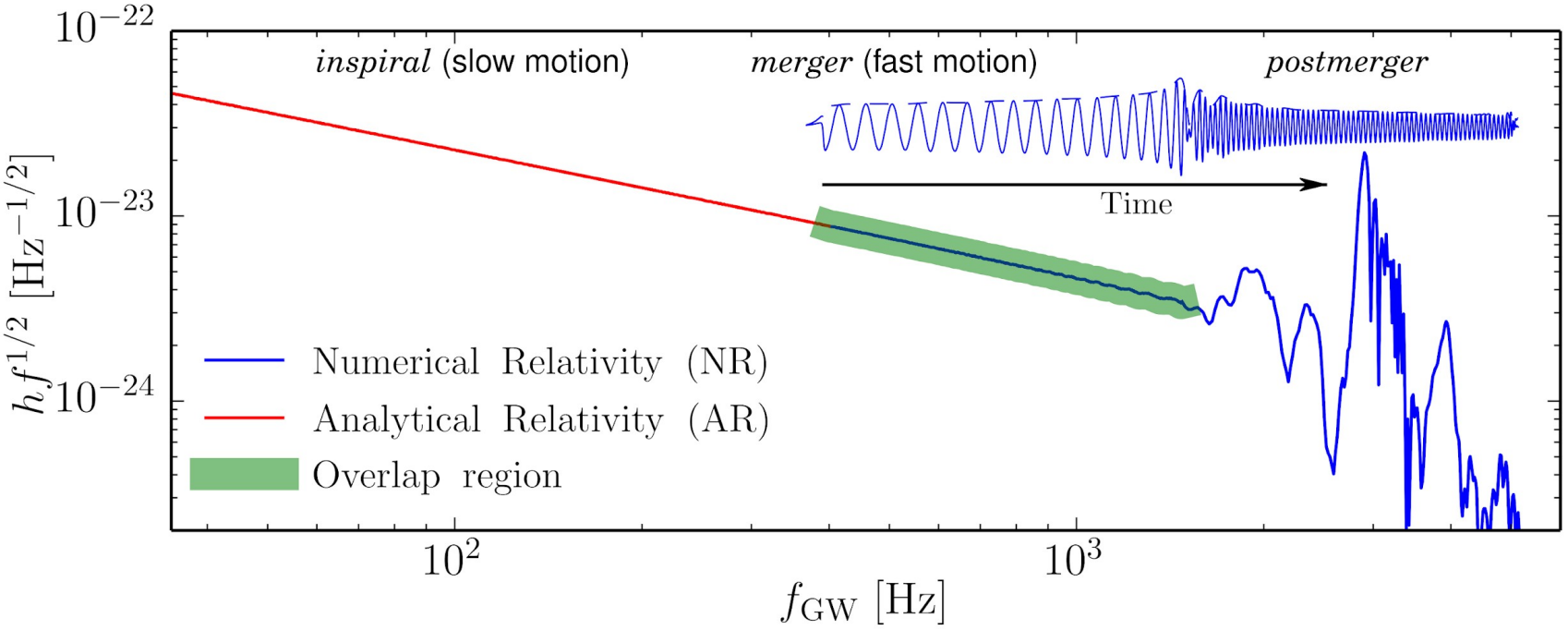

The complete GW spectrum

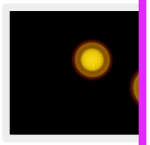

Central challenge: model tidal interactions (short-range/high-frequency)
Carry imprint of equation of state via a multipolar set of
gravitoelectric and gravitomagnetic tidal polarizability parameters

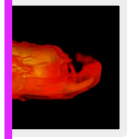

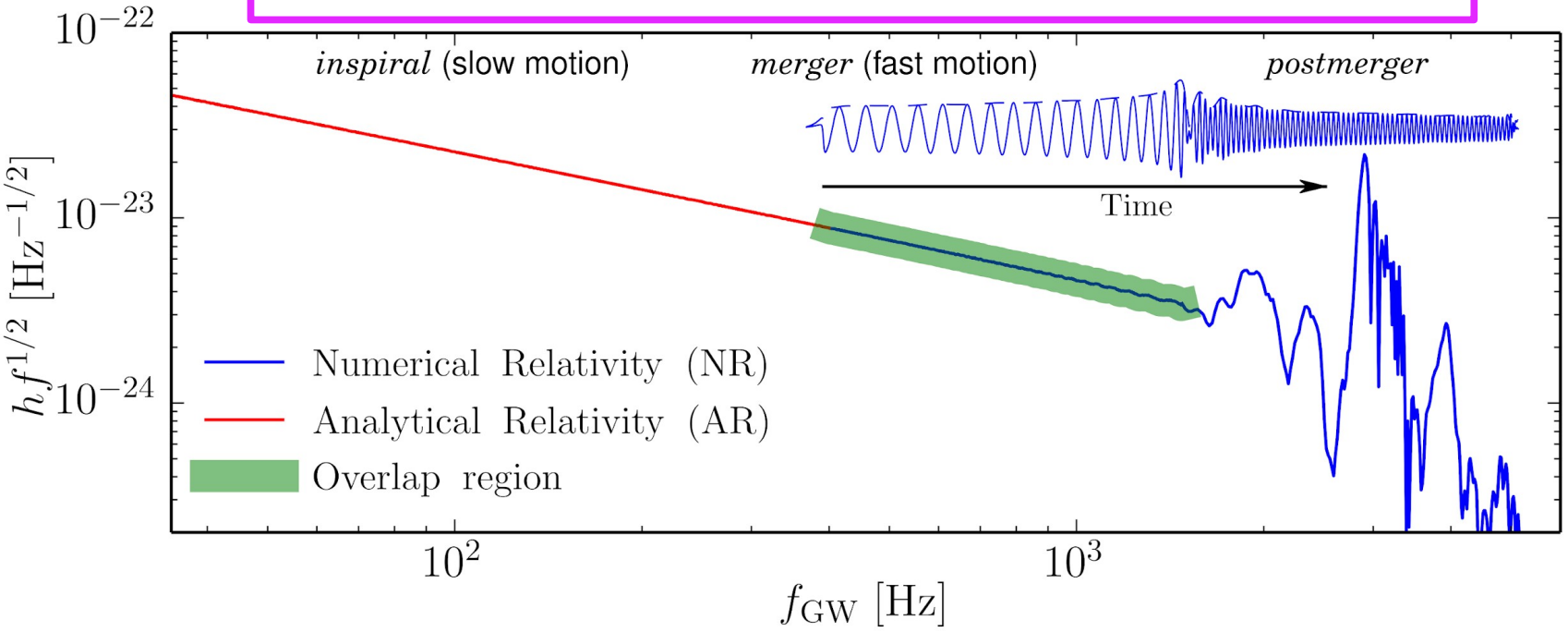

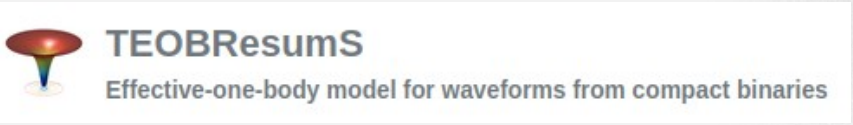

- **Effective one body approach to GR 2-body problem**
  - Map GR Hamiltonian in effective one [*Buonanno&Damour 2000*]
  - Includes test-mass limit by design
  - Includes post-Newtonian and self-force results
  - Factorized (resummed) PN waveform [*Damour,Iyer,Nagar 2008*]
  - Resummation techniques → predictive strong-field regime
  - Includes tidal interactions (→ BNS) [*Damour&Nagar 2010*]
  - Flexible framework → NR informed

- **Latest release: Dalí** [*Albanesi+ 2025*]
  - Generic motion: bound (circular,eccentric) and hyperbolic orbits (dynamical captures & scattering)
  - Generic binaries: spin & tidal interactions, postmerger completion, arbitrary length & mass ratio (e.g. EMRIs)

- **Example application:** GW190521 as a dynamical capture of two nonspinning black holes *[Gamba+ Nature Astronomy 2021]*

Effective-one-body framework in a nutshell

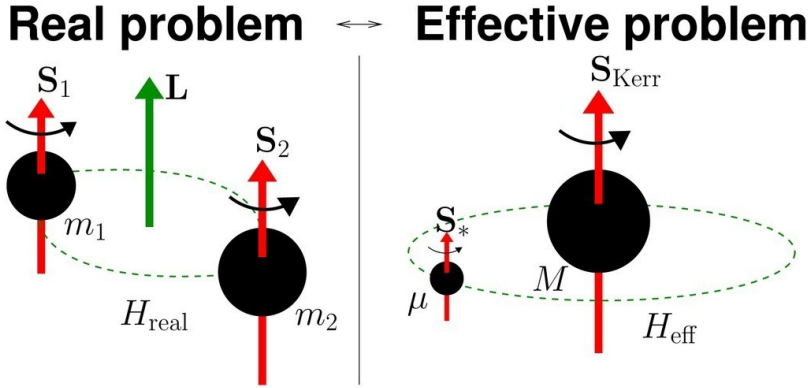

Credit: A.Taracchini

$$H_{\rm eff} \sim \mu \sqrt{A(u)(1+p_\phi^2 u^2) + p_{r^*}^2}$$

$$A(u;\nu;\kappa_2^T) = A^0(u;\nu) + A^T(u;\nu;\kappa_2^T)$$

$$A^0(u;\nu) = 1 - 2u + \nu(...$$

Factorized (resummed) PN waveform [Damour,Iyer,Nagar 2008]
Includes test-mass limit (i.e. particle on Schwarzschild)
Includes post-Newtonian and self-force results
Uses resummation techniques → predictive strong-field regime
Includes tidal interactions (→ BNS) [Damour&Nagar PRD 2010]
Flexible framework → NR informed

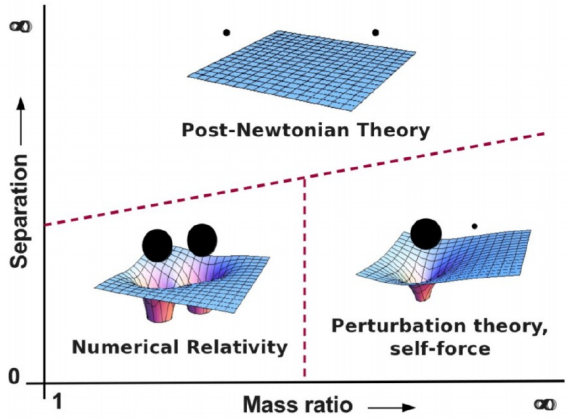

Credit: L.Barak

Tidal interactions in BNS

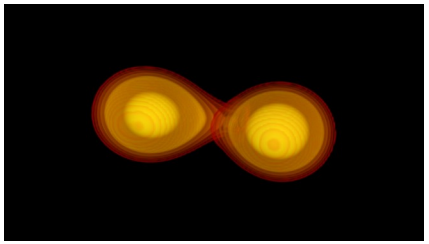

$$\kappa_2^{\mathrm{T}} = \frac{3}{2}\left[\Lambda_2^{\mathrm{A}} X_{\mathrm{A}}^4 X_{\mathrm{B}} + \Lambda_2^{\mathrm{B}} X_{\mathrm{B}}^4 X_{\mathrm{A}}\right]$$

[Damour&Nagar 2009b]

(Note $\bar{\Lambda}$ has a different expression, but same meaning)

"Tidal coupling constant"

Hamiltonian (Newtonian limit):

$$H_{\mathrm{EOB}} \approx Mc^2 + \frac{\mu}{2}\left(\mathbf{p}^2 + A(r) - 1\right)$$

$$A(r) = 1 - 2/r - \kappa_2^T(\lambda_2)/r^6$$

Tides are attractive and short range

Waveform:

$$h \sim A f^{-7/6} e^{-i\Psi(f)} \approx A f^{-7/6} e^{-i\Psi_{PP}(f) + i39/4\kappa_2^T x(f)^{5/2}}$$

Key point: No other binary parameter (mass, radii, etc) enter separately the formalism at LO

Tidal polarizability coefficients

Encode EOS and compactness

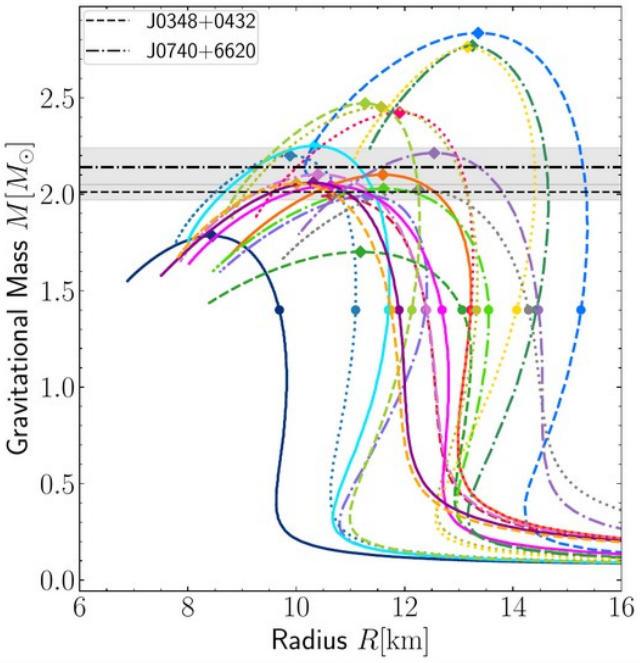

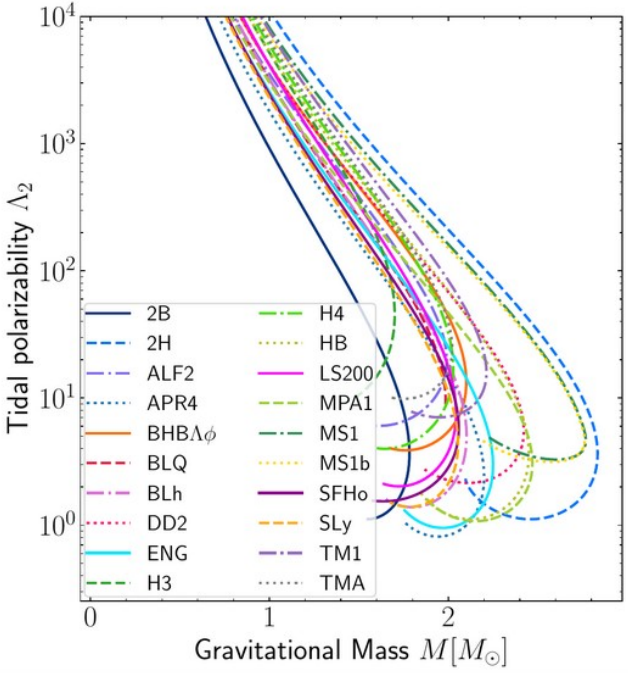

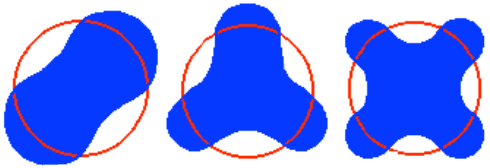

Love numbers:

$$Q_{ij} = \lambda_2 G_{ij} \sim \lambda_2 \partial_i \partial_j \phi$$

Tidal pol. coef:

$$\Lambda_2 = \frac{2}{3}\,\lambda_2 \left(\frac{M}{R}\right)^5$$

kHertz GWs: NR-informed postmerger completion

PRL 115, 091101 (2015) PHYSICAL REVIEW LETTERS week ending 28 AUGUST 2015

Modeling the Complete Gravitational Wave Spectrum of Neutron Star Mergers

Sebastiano Bernuzzi,[1,2] Tim Dietrich,[3] and Alessandro Nagar[4]
[1]*TAPIR, California Institute of Technology, 1200 East California Boulevard, Pasadena, California 91125, USA*
[2]*DiFeST, University of Parma and INFN Parma, I-43124 Parma, Italy*
[3]*Theoretical Physics Institute, University of Jena, 07743 Jena, Germany*
[4]*Institut des Hautes Etudes Scientifiques, 91440 Bures-sur-Yvette, France*
(Received 9 April 2015; revised manuscript received 11 June 2015; published 27 August 2015)

- Quasiuniversal (EOS-insensitive) relations w/ tidal coupling constant
  SB+ [https://arxiv.org/abs/1504.01764]
- First complete spectrum model
  (EOB completion with NRPM)
  Breschi+ [https://arxiv.org/abs/1908.11418]
- Improved frequency domain NRPMw
  Breschi+ [https://arxiv.org/abs/2205.09112]

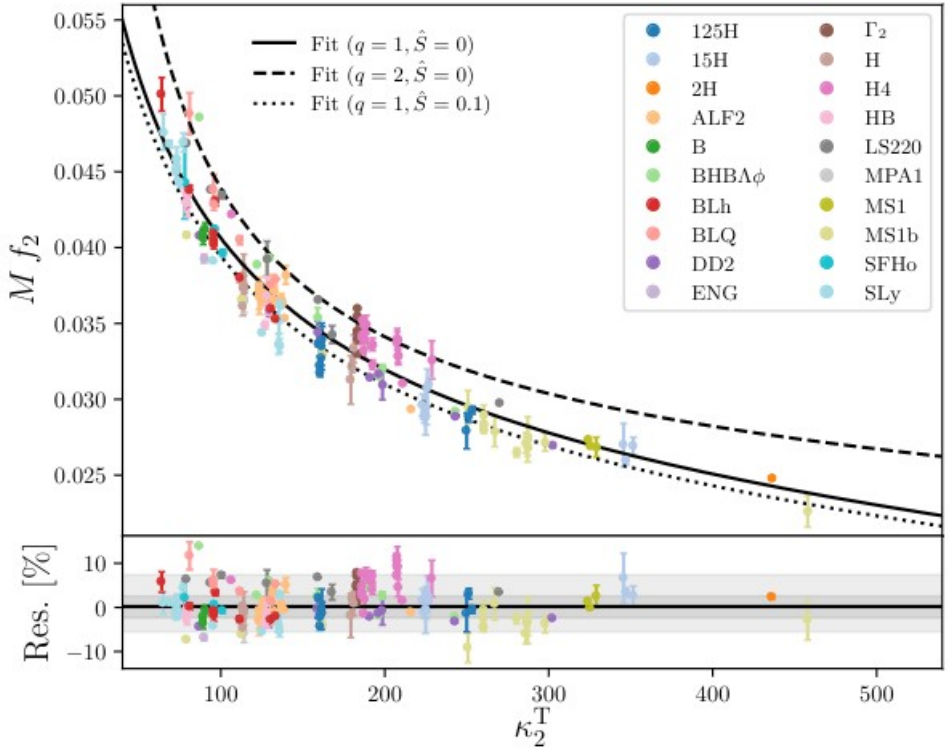

kHertz GWs: NR-informed postmerger completion

PRL 115, 091101 (2015) PHYSICAL REVIEW LETTERS week ending 28 AUGUST 2015

Modeling the Complete Gravitational Wave Spectrum of Neutron Star Mergers

Sebastiano Bernuzzi,[1,2] Tim Dietrich,[3] and Alessandro Nagar[4]
[1]*TAPIR, California Institute of Technology, 1200 East California Boulevard, Pasadena, California 91125, USA*
[2]*DiFeST, University of Parma and INFN Parma, I-43124 Parma, Italy*
[3]*Theoretical Physics Institute, University of Jena, 07743 Jena, Germany*
[4]*Institut des Hautes Etudes Scientifiques, 91440 Bures-sur-Yvette, France*
(Received 9 April 2015; revised manuscript received 11 June 2015; published 27 August 2015)

- Quasiuniversal (EOS-insensitive) relations w/ tidal coupling constant
  SB+ [https://arxiv.org/abs/1504.01764]
- First complete spectrum model (EOB completion with NRPM)
  Breschi+ [https://arxiv.org/abs/1908.11418]
- Improved frequency domain NRPMw
  Breschi+ [https://arxiv.org/abs/2205.09112]

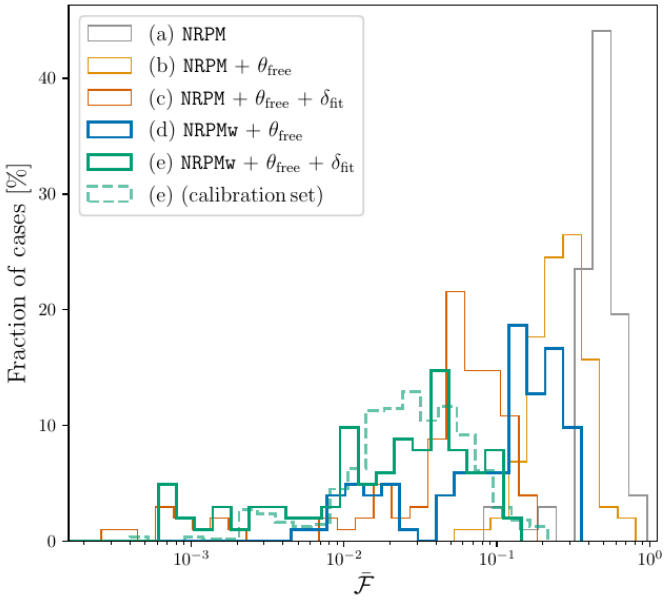

FIG. 5. Recovered unfaithfulness $\bar{\mathcal{F}}$ between PM models and NR data of the validation set [11, 55, 61, 72, 88, 110] employing ET-D sensitivity [2, 3]. For NRPM [11] (thin lines), we compute $\bar{\mathcal{F}}$ with the standard model (a), including PM parameters (b) and also the recalibrations (c). Analogously, the $\bar{\mathcal{F}}$ recovered for NRPMw (thick lines) include the PM parameters (d) and also the recalibrations (e). The dashed histogram shows the $\bar{\mathcal{F}}$ for case (e) computed over the calibration set.

Public data release

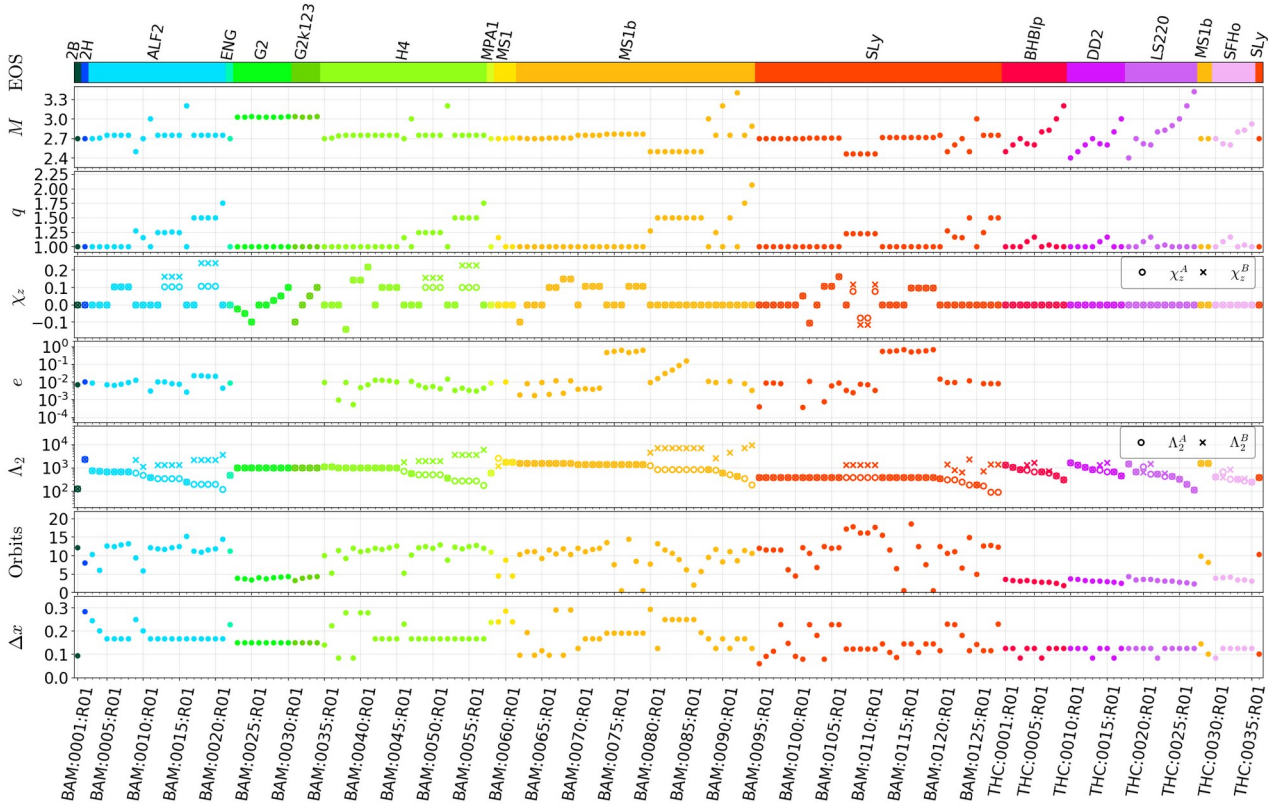

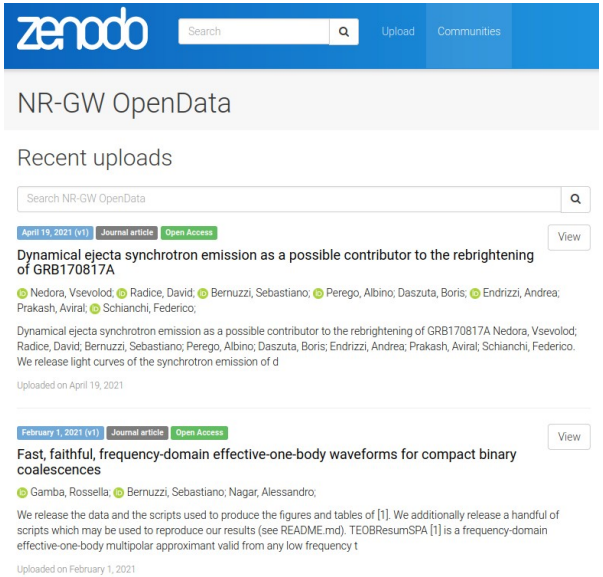

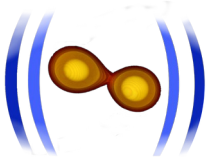

CoRe www.computational-relativity.org

Full-spectrum constraints w/ Einstein Telescope

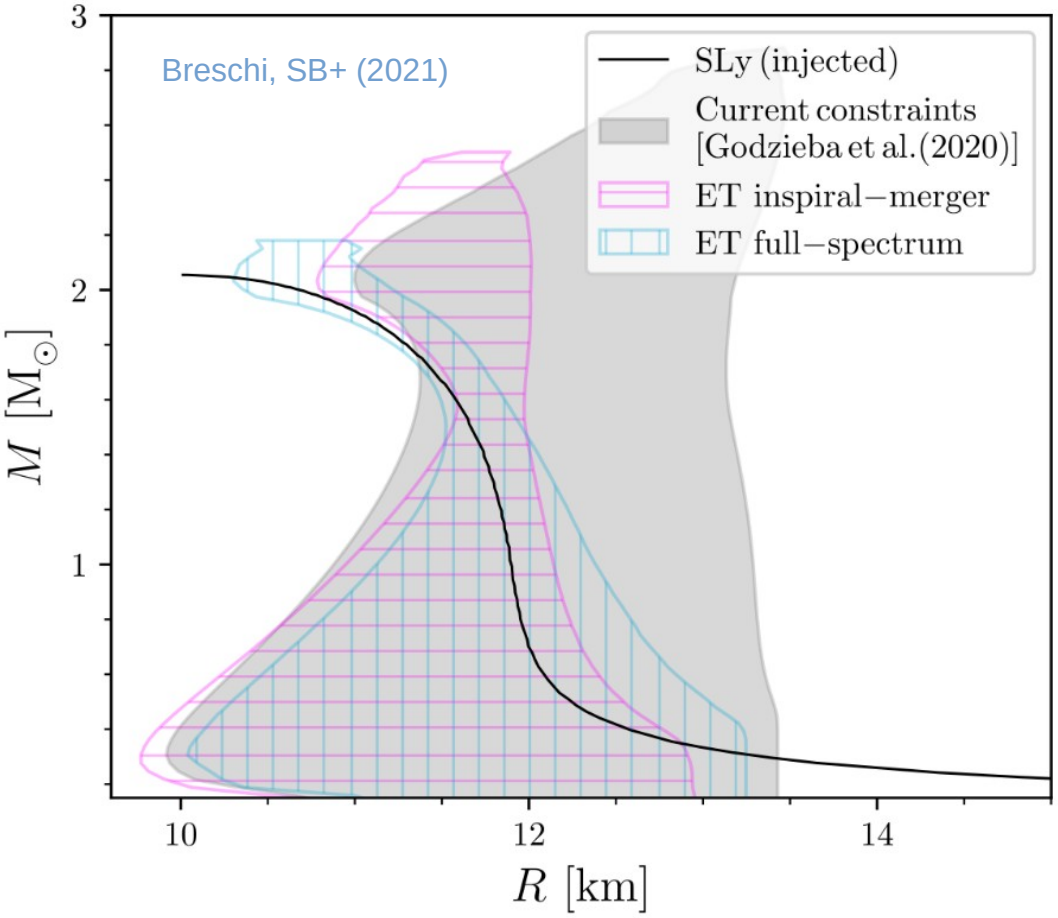

- Full-spectrum mock analysis of single event @ minimum SNR threshold for postmerger detection

  NB SNR(PM)~8 vs. SNR(IM)~1000

- Postmerger signal helps constraining full stable branch of mass-radius diagram

- EOS sampling from 2 million piecewise polytropes with minimal hypothesis (causality, GR)
  + current constraints from previous slide

Full-spectrum constraints w/ Einstein Telescope

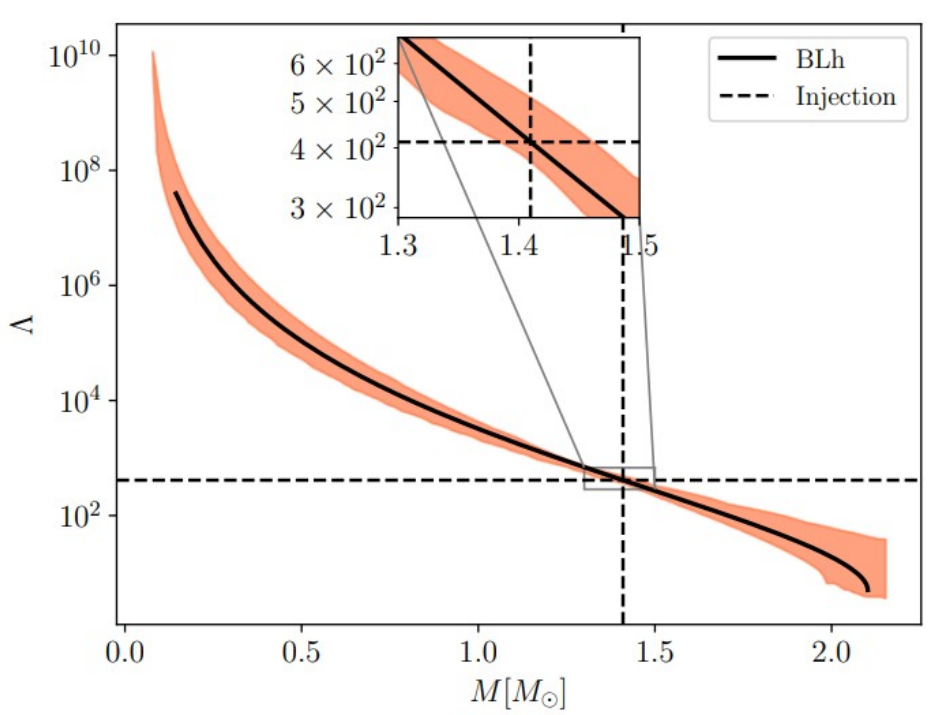

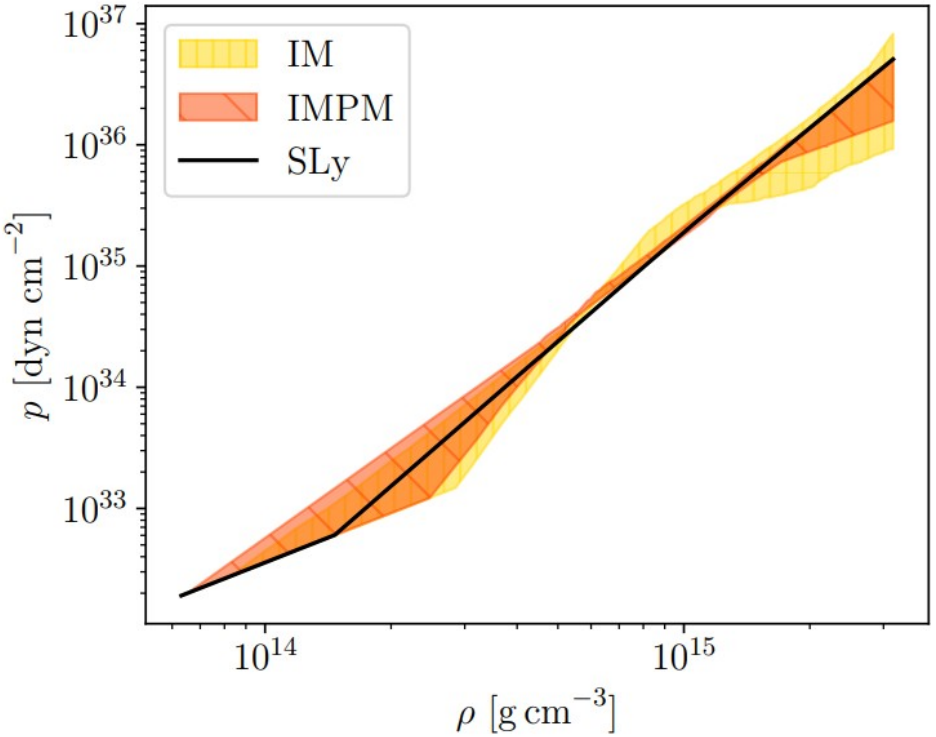

Quadrupolar tidal polarizability – mass curve | pressure – mass density curve

Huez, SB+ (2024)

Einstein Telescope sensitivity to kHz GWs

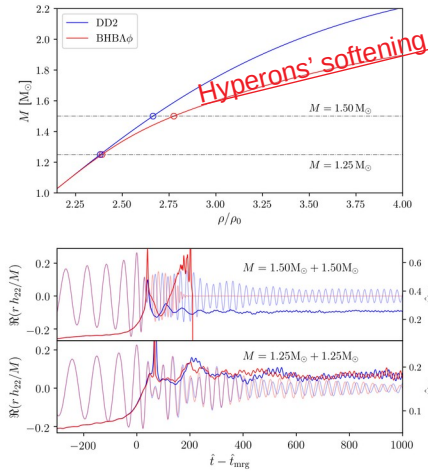

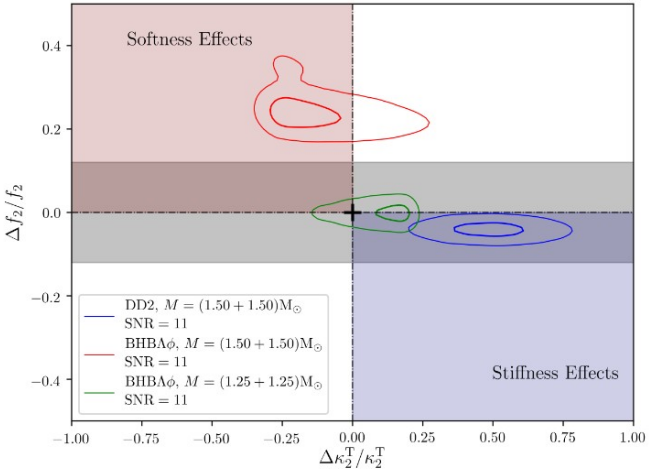

"EOS Softness" (Hyperons, phase transitions,…)

Effect of hyperonic d.o.f. at remnant densities:
→ pressure support reduces w.r.t hadronic
→ more compact remnant or black hole formation

Radice, SB+ [https://arxiv.org/abs/1612.06429]
Breschi, SB+ [https://arxiv.org/abs/1908.11418]
Breschi+ [https://arxiv.org/abs/2301.09672]

"Thermal effects" (effective nucleon mass)

Increasing effective nucleon mass:
→ specific heat increases
→ thermal pressure support reduces
→ the remnants become colder and more compact

Fields+ [https://arxiv.org/abs/2302.11359]

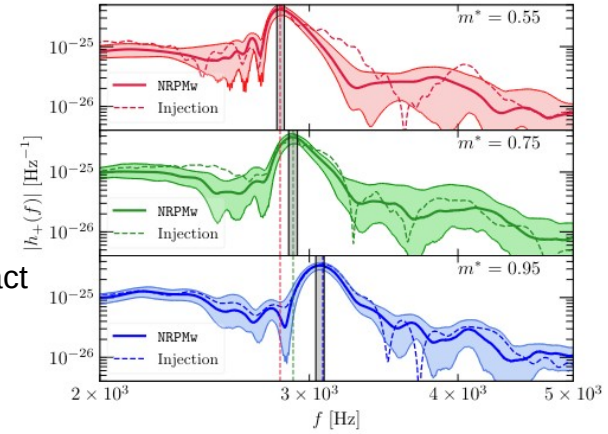

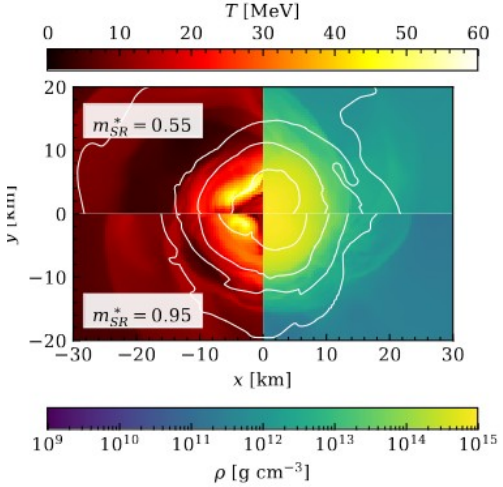

Einstein Telescope sensitivity to kHz GWs

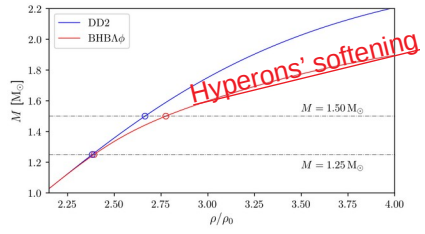

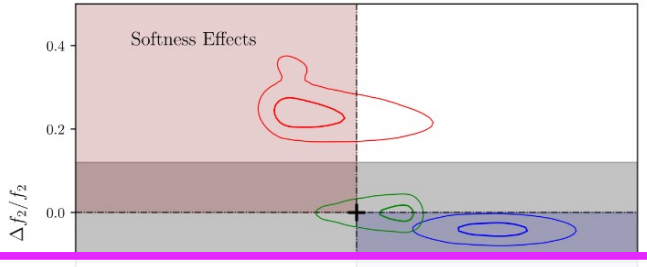

"EOS Softness" (Hyperons, phase transitions,…)

Effect of hyperonic d.o.f. at remnant densities:
→ pressure support reduces w.r.t hadronic
→ more compact remnant or black hole formation

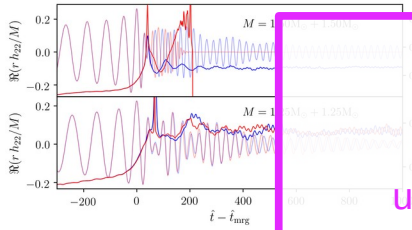

How to actually detect these effects after a real event?
"real EOS" is unknown, candidate EOS are uncountable
Degenerate effects
uncertainties in empirical quasi-universal relations hard to quantify

Radice, SB+ [https://arxiv.org/abs/1612.06429]
Bresseni, SB+ [https://arxiv.org/abs/1908.11418]
[https://arxiv.org/abs/2301.09672]

"Thermal effects" (effective nucleon mass)

Increasing effective nucleon mass:
→ specific heat increases
→ thermal pressure support reduces
→ the remnants become colder and more compact

Fields+ [https://arxiv.org/abs/2302.11359]

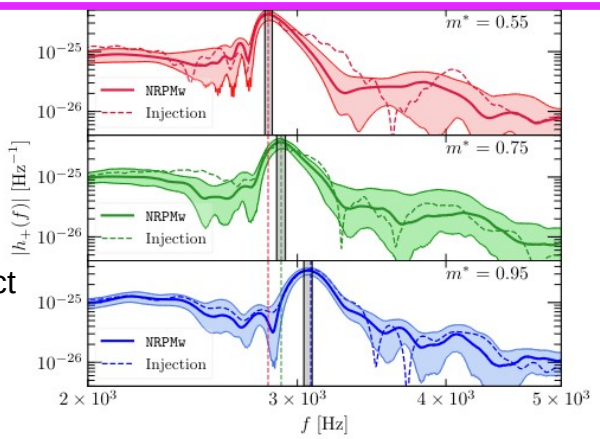

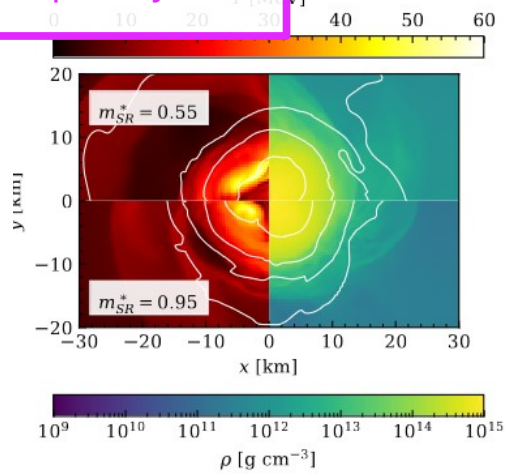

Systematics & waveform accuracy

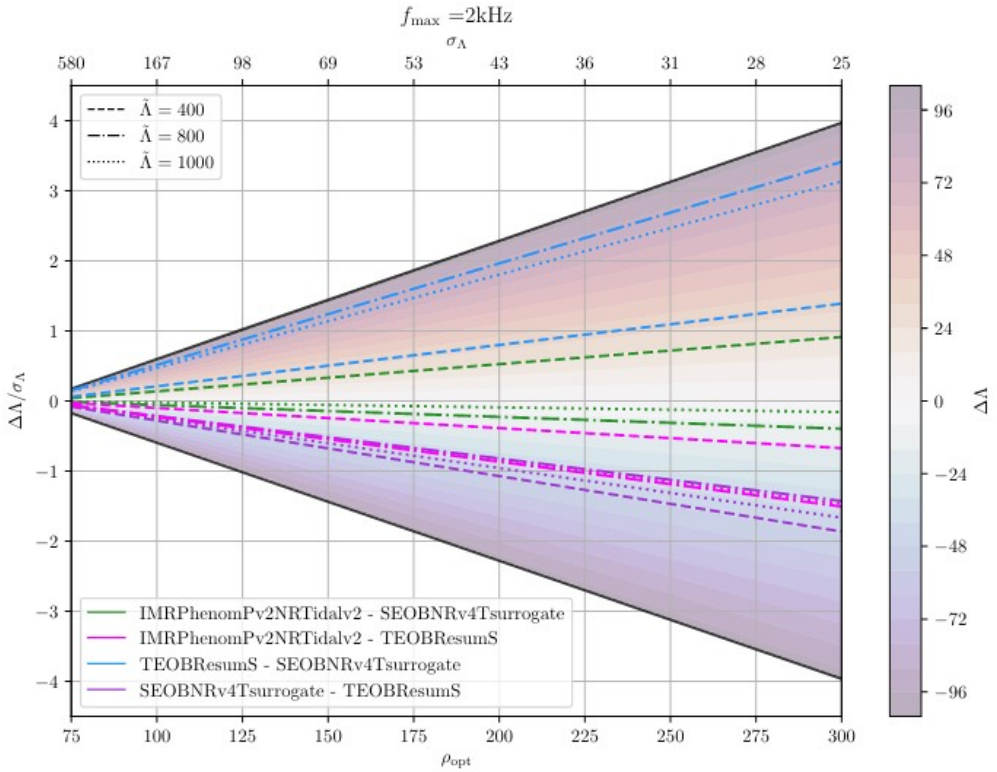

TABLE V. Faithfulness values $\mathcal{F}$ computed considering frequencies from $f_{\rm low}$ to $f_{\rm mrg}$ between simulations with the same intrinsic parameters and two different resolutions, extracted at $r/M = 1000$. The source is situated in the same sky location as GW170817, and the waveform polarizations h_+ and $h_\times$ are computed and projected on the Livingston detector. We employ the `aLIGODesignSensitivityP1200087` [22] PSD from `pycbc` [110] to compute the matches, and compare the values obtained to the thresholds $\mathcal{F}_{\rm thr}$ calculated with Eq. 19 with $\epsilon^2 = 1$ or $\epsilon^2 = N$. A tick ✓ indicates that $\mathcal{F} > \mathcal{F}_{\rm thr}$. Conversely, a cross ✗ indicates that $\mathcal{F} < \mathcal{F}_{\rm thr}$.

Sim	n[a]	$\mathcal{F}$	SNR					
			14		30		80	
			$N=6$	1	$N=6$	1	$N=6$	1
BAM:0011	[96, 64]	0.991298	✓	✗	✗	✗	✗	✗
BAM:0017	[96, 64]	0.985917	✓	✗	✗	✗	✗	✗
BAM:0021	[96, 64]	0.957098	✗	✗	✗	✗	✗	✗
BAM:0037	[216, 144]	0.998790	✓	✓	✓	✗	✗	✗
BAM:0048	[108, 72]	0.983724	✗	✗	✗	✗	✗	✗
BAM:0058	[64, 64]	0.999127	✓	✓	✓	✗	✗	✗
BAM:0064	[240, 160]	0.997427	✓	✗	✓	✗	✗	✗
BAM:0091	[144, 108]	0.997810	✓	✓	✓	✗	✗	✗
BAM:0094	[144, 108]	0.996804	✓	✗	✓	✗	✗	✗
BAM:0095	[256, 192]	0.999550	✓	✓	✓	✓	✓	✗
BAM:0107	[128, 96]	0.995219	✓	✗	✗	✗	✗	✗
BAM:0127	[128, 96]	0.999011	✓	✓	✓	✗	✗	✗

[a] Number of grid point (linear resolution) of the finest grid refinement, roughly covering the diameter of one NS

Gamba,Breschi,SB+ [https://arxiv.org/abs/2009.08467]

Systematics & waveform accuracy

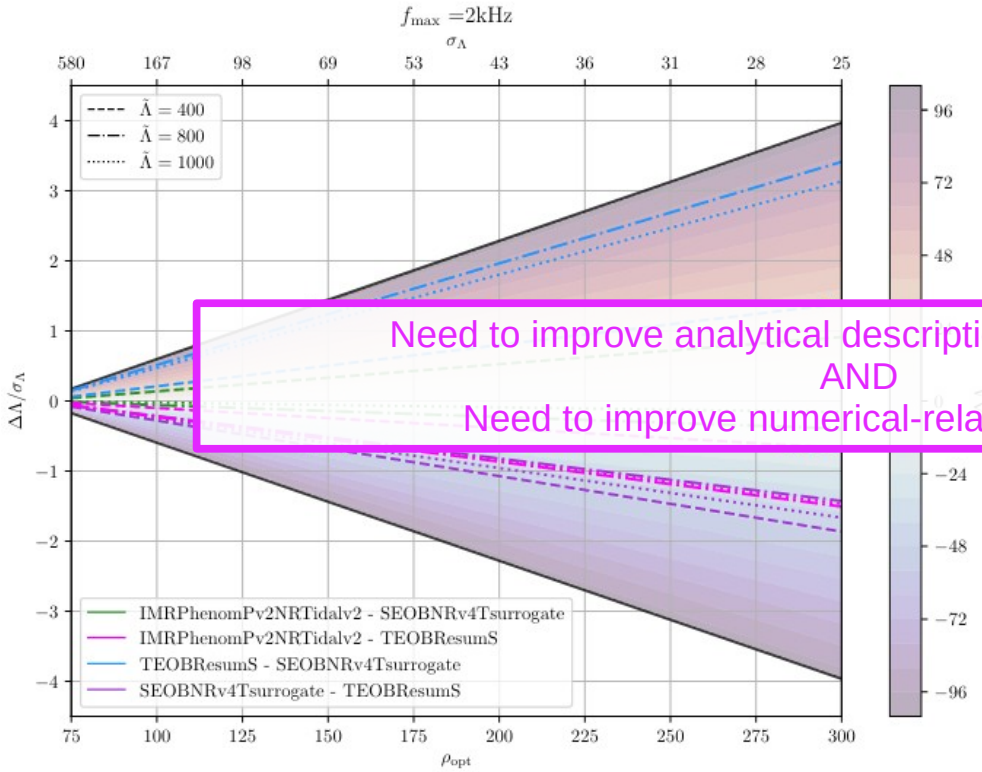

Need to improve analytical description of tidal interaction
AND
Need to improve numerical-relativty data quality

TABLE V. Faithfulness values $\mathcal{F}$ computed considering frequencies from $f_{\rm low}$ to $f_{\rm mrg}$ between simulations with the same intrinsic parameters and two different resolutions, extracted at $r/M = 1000$. The source is situated in the same sky location as GW170817, and the waveform polarizations h_+ and $h_\times$ are computed and projected on the Livingston detector. We employ the `aLIGODesignSensitivityP1200087` [22] PSD from `pycbc` [110] to compute the matches, and compare the values obtained to the thresholds $\mathcal{F}_{\rm thr}$ calculated with Eq. 19 with $\epsilon^2 = 1$ or $\epsilon^2 = N$. A tick ✓ indicates that $\mathcal{F} > \mathcal{F}_{\rm thr}$. Conversely, a cross ✗ indicates that $\mathcal{F} < \mathcal{F}_{\rm thr}$.

			SNR					
			30				80	
			$N = 6$	1	$N = 6$	1	$N = 6$	1
BAM:0021	[96, 64]	0.957098	✗	✗	✗	✗	✗	✗
BAM:0037	[216, 144]	0.998790	✓	✓	✓	✗	✗	✗
BAM:0048	[108, 72]	0.983724	✗	✗	✗	✗	✗	✗
BAM:0058	[64, 64]	0.999127	✓	✓	✓	✗	✗	✗
BAM:0064	[240, 160]	0.997427	✓	✗	✓	✗	✗	✗
BAM:0091	[144, 108]	0.997810	✓	✓	✓	✗	✗	✗
BAM:0094	[144, 108]	0.996804	✓	✗	✓	✗	✗	✗
BAM:0095	[256, 192]	0.999550	✓	✓	✓	✓	✓	✗
BAM:0107	[128, 96]	0.995219	✓	✗	✗	✗	✗	✗
BAM:0127	[128, 96]	0.999011	✓	✓	✓	✗	✗	✗

[a] Number of grid point (linear resolution) of the finest grid refinement, roughly covering the diameter of one NS

Gamba,Breschi,SB+ [https://arxiv.org/abs/2009.08467]

Scattering of Two Neutron Stars

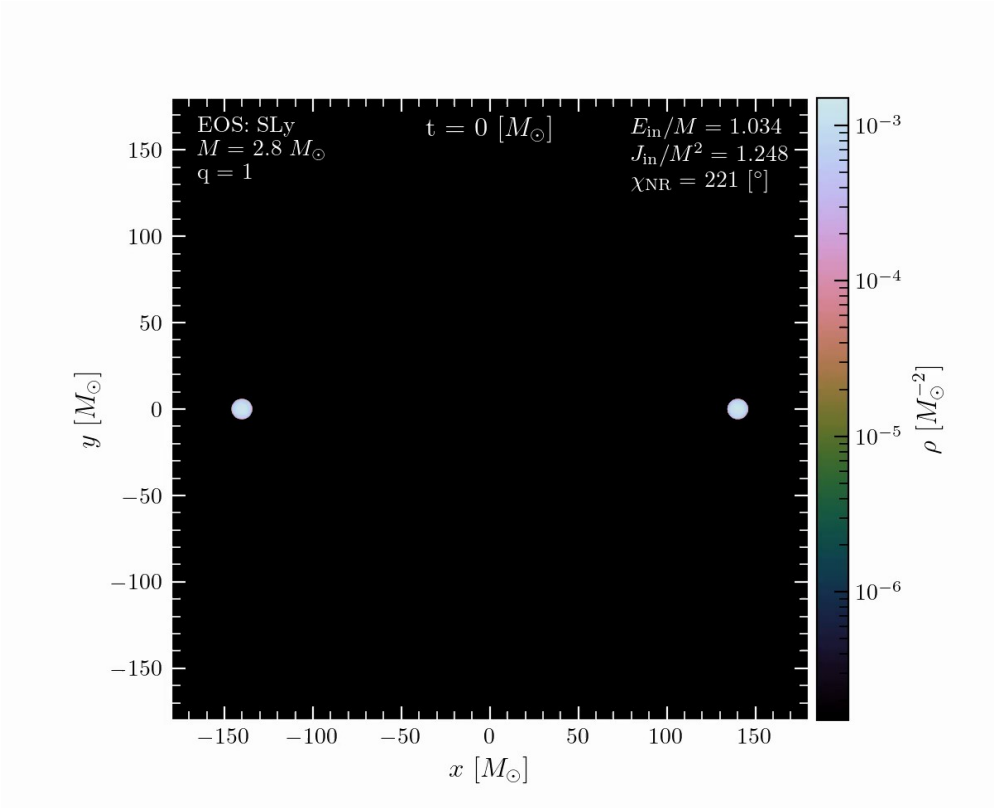

Fontebute, SB+ (2025)

Scattering of Two Neutron Stars

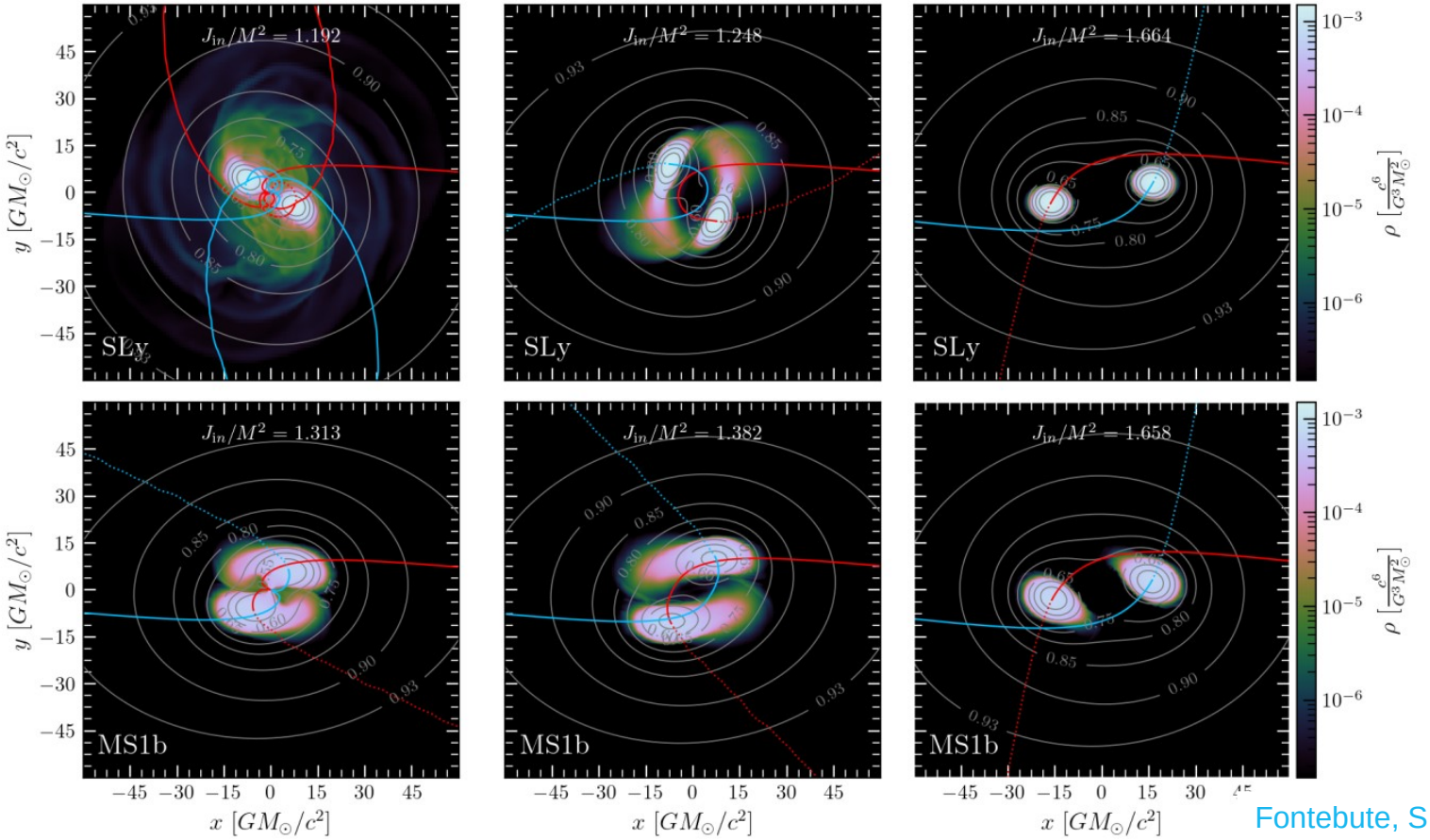

Fontebute, SB+ (2025)

Scattering angle and perturbative predictions

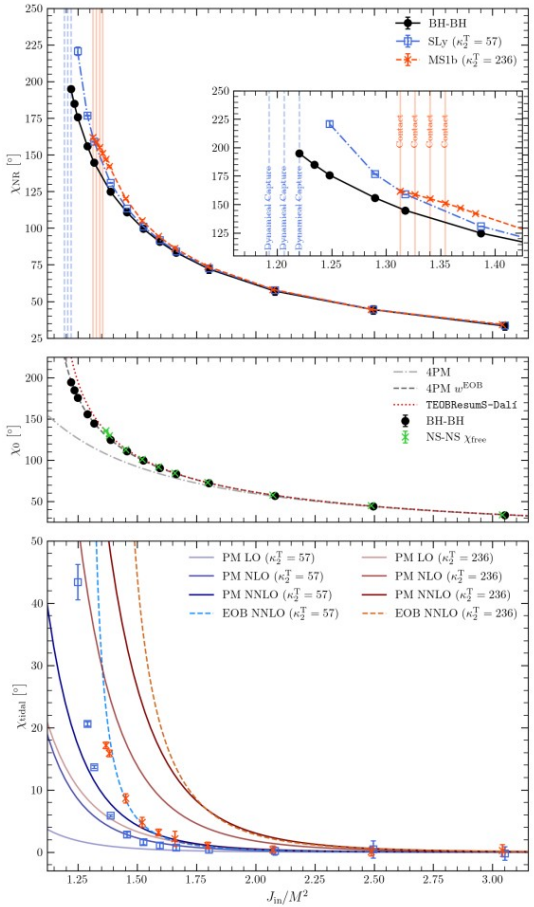

- Fixed “in” energy and varying “in” angular momentum
- Two sequences: SLy “soft” and MS1b “stiff” EOS
- “Tidal free” contribution compatible with BH-BH scattering
- BH-BH term requires EOB-resummation of Post-Minkowskian computations [Damour&Rettegno 2022]
- Tidal contribution significantly differ from EOB and Post-Minkowskian computations (@ NNLO) towards dynamical capture threshold
  → higher order computation + resummation ?
- Transition to bound motion aided by significant mass ejecta, unbound rest mass ~ 1Mo
  → EM counterparts & rate constraints [Rosswog+ 2019]

Fontebute, SB+ (2025)

Mass ejecta & nucleosynthesis

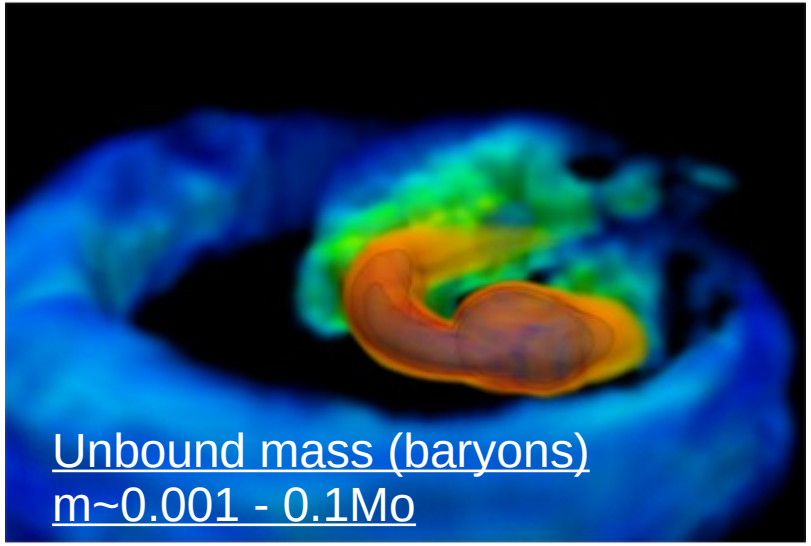

NS-BH collisions (1974) Decompression of cold neutron star matter

D. Schramm, J. Lattimer, D. Eichler, T. Piran, F. Thielemann, and ...
… many others

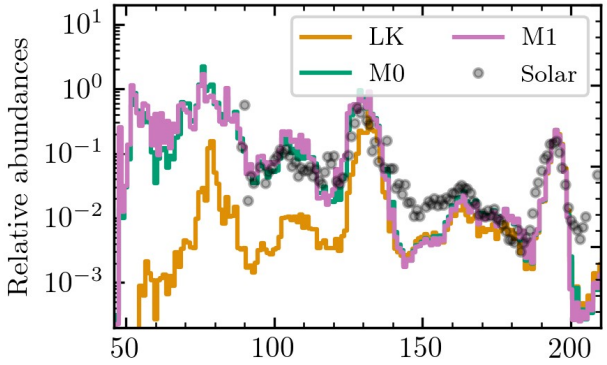

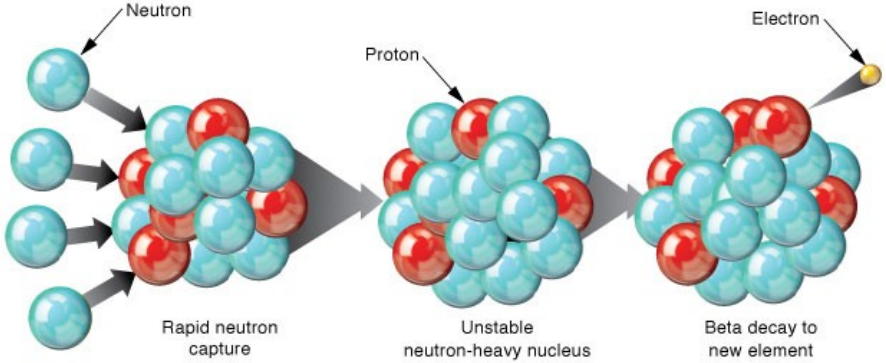

Radioactive heating & thermalization (β-decays, α-decays, fission)

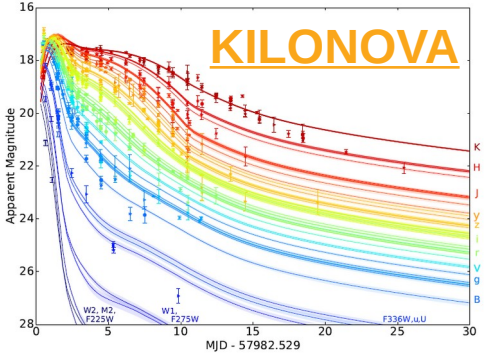

Mass outflows: multi-scale & multi-physics

- Dynamical ejecta
  GW driven phase, merger timescales ~few msec
  m ~ 10^{-3} Mo, v ~ 0.3 - 0.6 c
  Tidal & Shock-heated components

- Spiral-wave winds
  GW/viscous driven phase, timescales ~10-100 msec
  m ~ 10^{-3} - 10^{-2} Mo, v ~ 0.1 - 0.4 c
  Hydrodynamics (+neutrinos, +MHD)

- Neutrino- & MHD- turbulence driven disk winds
  viscous phase 0.1 - 1+ sec
  m ~ 10^{-2} - 10^{-1} Mo, v ~ 0.1 c
  Long-term evolution & nuclear heating

- Jet (~1+ sec)
  Injection mechanism (MHD & neutrinos) + remnant jet dynamics & particles acceleration

$t - t_{\rm mrg} = 0.6$ ms

Radice+ [https://arxiv.org/abs/1809.11161]

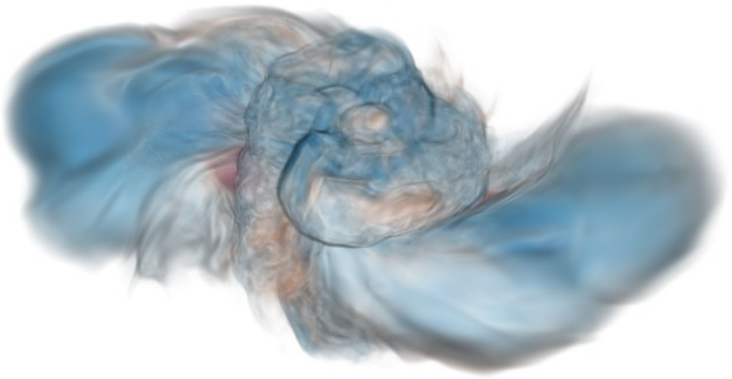

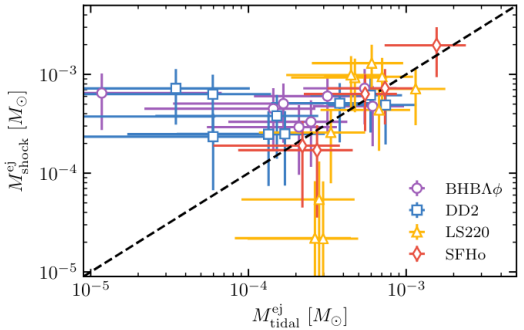

Mass outflows: multi-scale & multi-physics

- Dynamical ejecta
  GW driven phase, merger timescales ~few msec
  m ~ 10^{-3} Mo, v ~ 0.3 - 0.6 c
  Tidal & Shock-heated components

- Spiral-wave winds
  GW/viscous driven phase, timescales ~10-100 msec
  m ~ 10^{-3} - 10^{-2} Mo, v ~ 0.1 - 0.4 c
  Hydrodynamics (+neutrinos, MHD)

- Neutrino- & MHD- turbulence driven disk winds
  viscous phase 0.1 - 1+ sec
  m ~ 10^{-2} - 10^{-1} Mo, v ~ 0.1 c
  Long-term evolution?
  Nuclear heating, neutrino-dominated accretion

- Jet (~1+ sec)
  Injection mechanism (MHD & neutrinos) + remnant jet dynamics & particles acceleration

Nedora, SB+ [https://arxiv.org/abs/1907.04872]

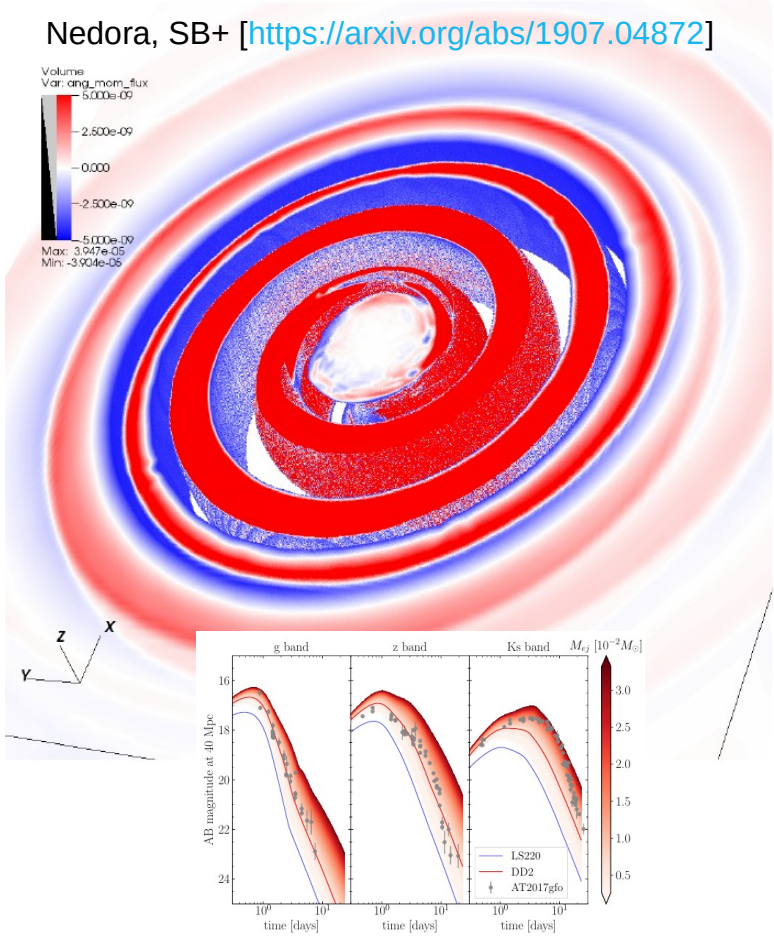

Mass outflows: multi-scale & multi-physics

- Dynamical ejecta
  GW driven phase, merger timescales ~few msec
  m ~ 10^{-3} Mo, v ~ 0.3 - 0.6 c
  Tidal & Shock-heated components

- Spiral-wave winds
  GW/viscous driven phase, timescales ~10-100 msec
  m ~ 10^{-3} - 10^{-2} Mo, v ~ 0.1 - 0.4 c
  Hydrodynamics (+neutrinos, MHD)

- Neutrino- & MHD- turbulence driven disk winds
  viscous phase 0.1 - 1+ sec
  m ~ 10^{-2} - 10^{-1} Mo, v ~ 0.1 c
  Long-term evolution?
  Nuclear heating, neutrino-dominated accretion

- Jet (~1+ sec)
  Injection mechanism (MHD & neutrinos) + remnant jet dynamics & particles acceleration

[Perego+ 2014]

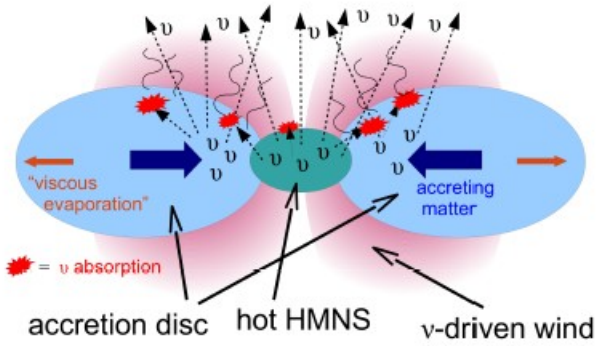

[Siegel+ 2014]

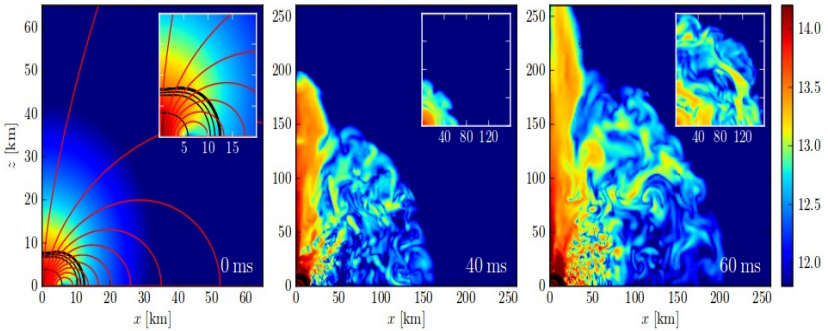

Mass outflows: multi-scale & multi-physics

- Dynamical ejecta
  GW driven phase, merger timescales ~few msec
  m ~ 10^{-3} Mo, v ~ 0.3 - 0.6 c
  Tidal & Shock-heated components

- Spiral-wave winds
  GW/viscous driven phase, timescales ~10-100 msec
  m ~ 10^{-3} - 10^{-2} Mo, v ~ 0.1 - 0.4 c
  Hydrodynamics (+neutrinos, MHD)

- Neutrino- & MHD- turbulence driven disk winds
  viscous phase 0.1 - 1+ sec
  m ~ 10^{-2} - 10^{-1} Mo, v ~ 0.1 c
  Long-term evolution?
  Nuclear heating, neutrino-dominated accretion

- Jet (~1+ sec)
  Injection mechanism (MHD & neutrinos) + remnant jet dynamics & particles acceleration

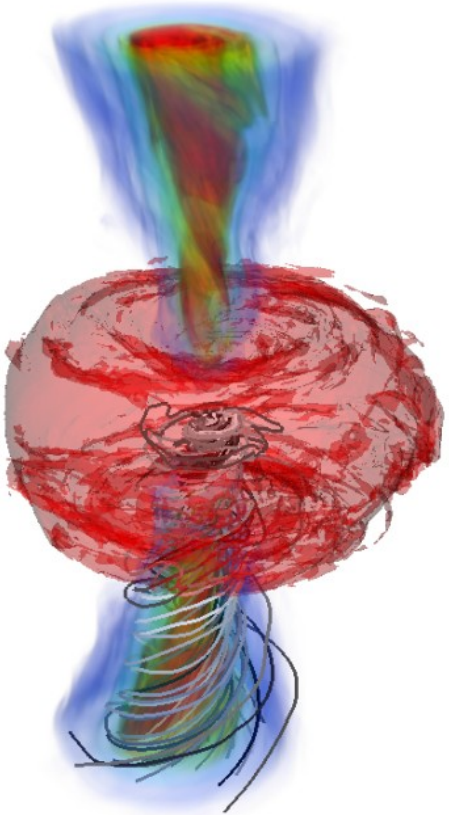

Moesta et al [https://arxiv.org/pdf/2003.06043]
(see also e.g. Kiuchi et al [https://arxiv.org/abs/2211.07637])

AT2017gfo & targeted simulations

Disc wind (upper limit)

w/ Spiral-wave wind

Dynamical ejecta

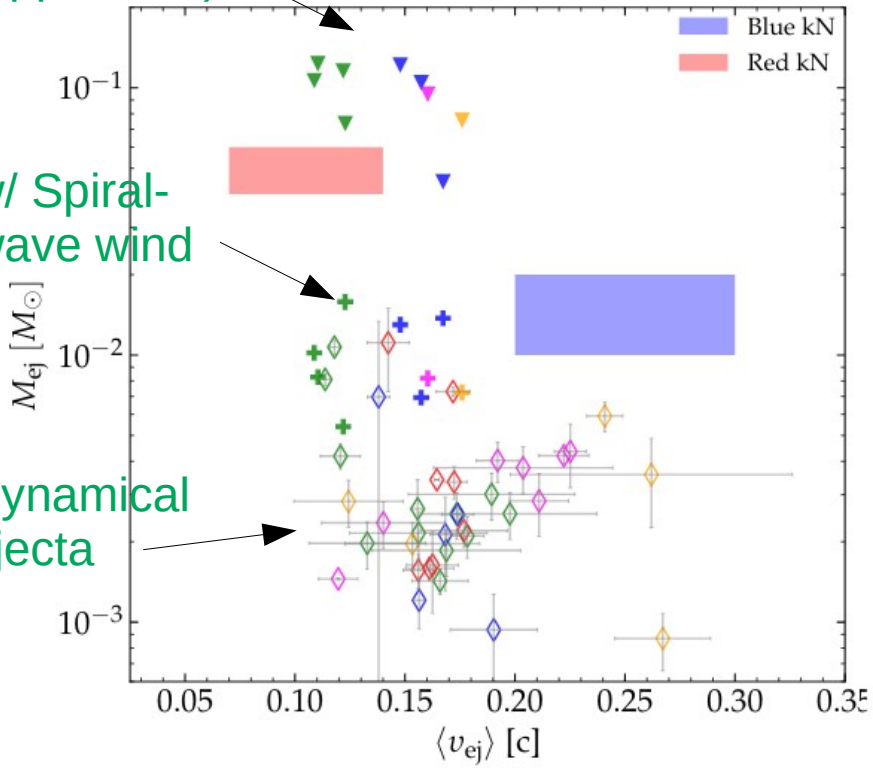

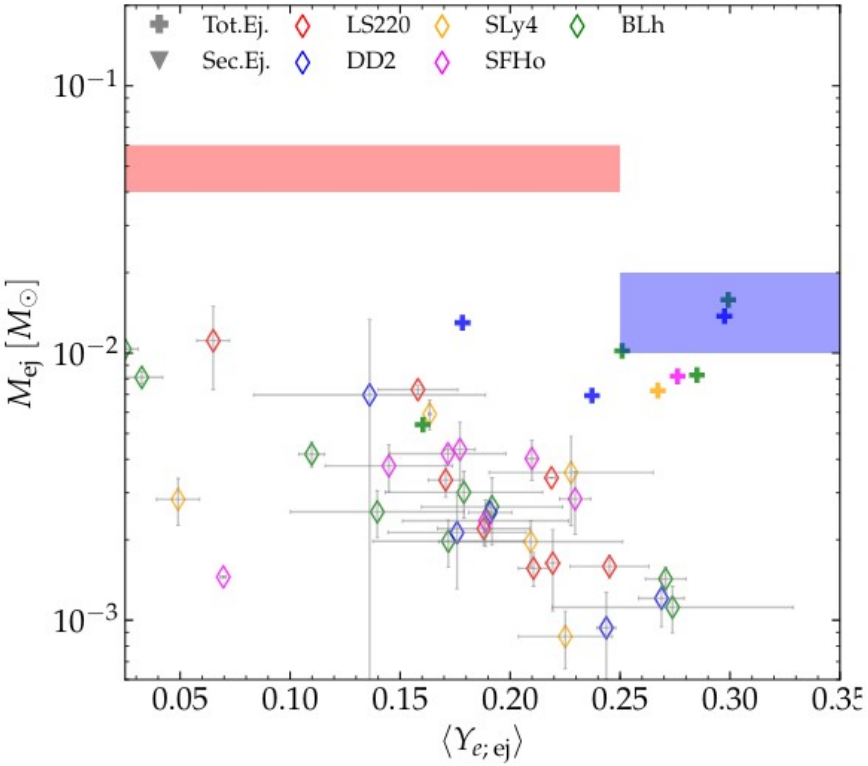

Nedora, SB+ [https://arxiv.org/pdf/2008.04333]

AT2017gfo & targeted simulations

Disc wind
(upper limit)

w/ Spiral-
wave wind

Dynamical
ejecta

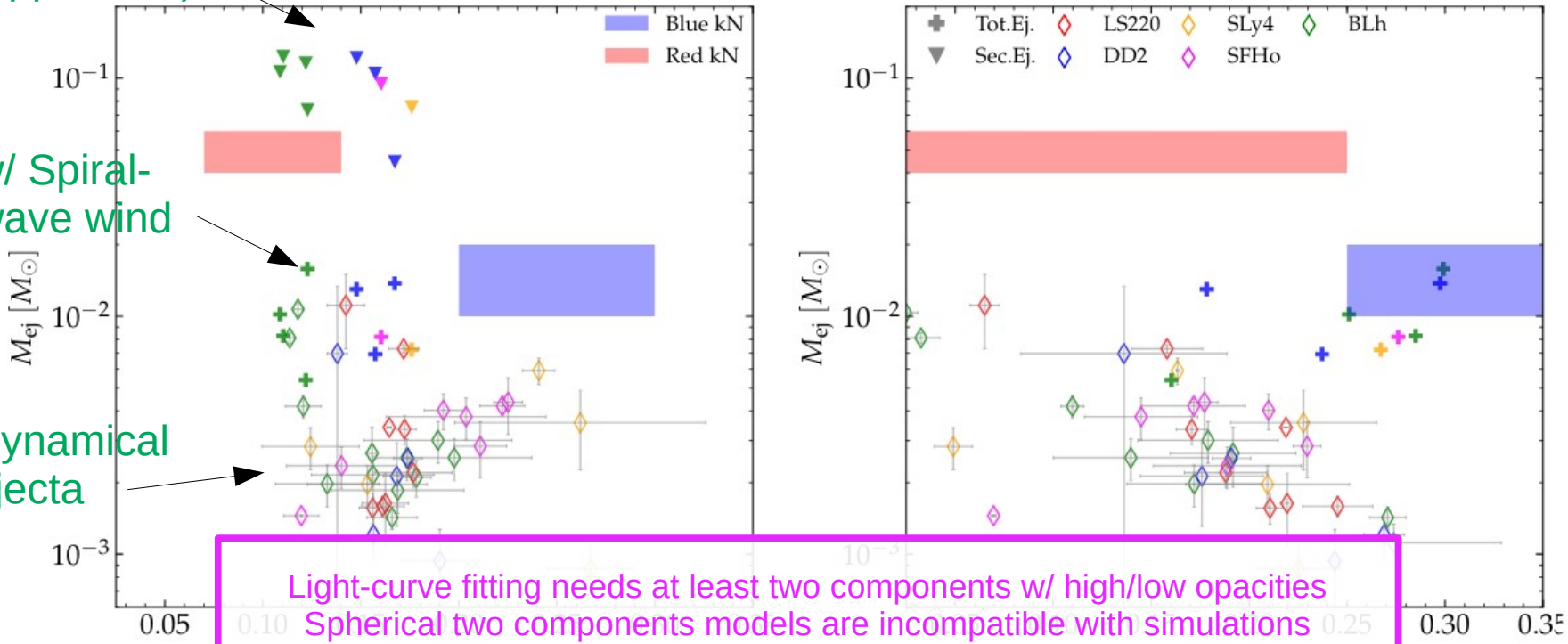

Light-curve fitting needs at least two components w/ high/low opacities
Spherical two components models are incompatible with simulations
Three anisotropic components are statistically favoured
(Bayesian model selection [Breschi+ 2021])

AT2017gfo & targeted simulations

Disc wind (upper limit)

w/ Spiral-wave wind

Dynamical ejecta

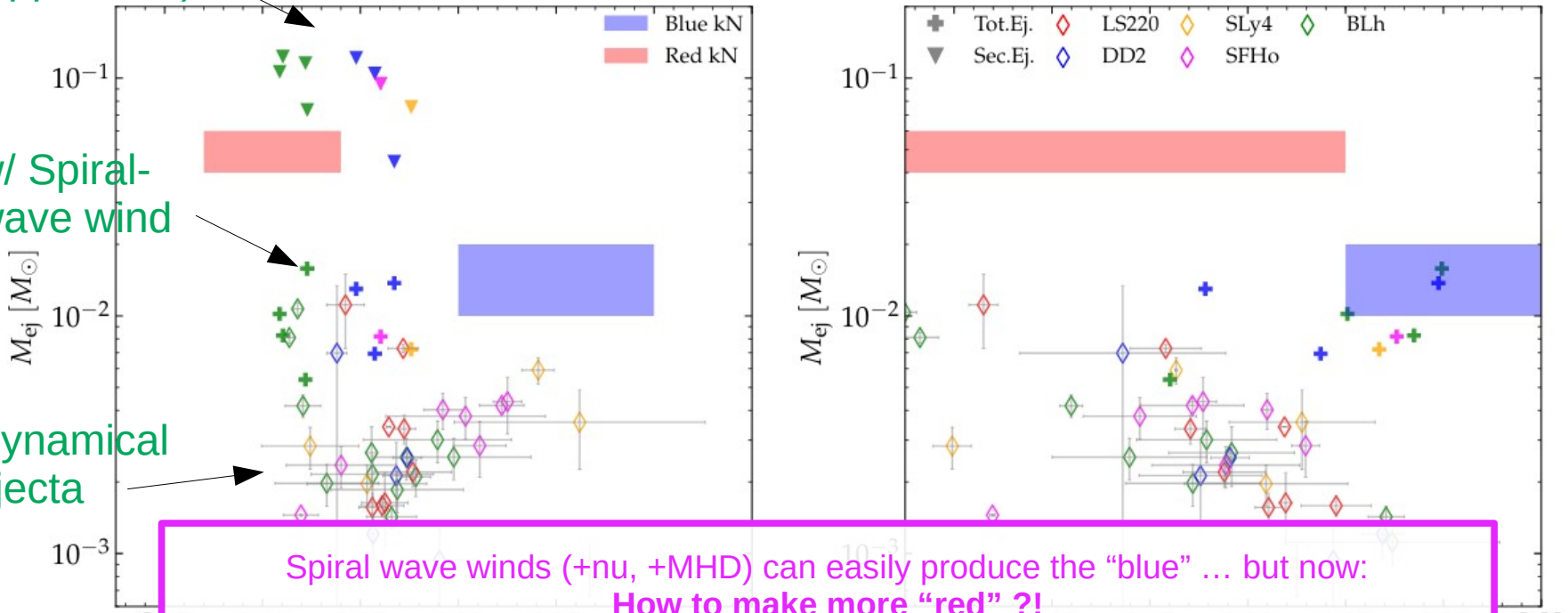

Spiral wave winds (+nu, +MHD) can easily produce the “blue” … but now:

How to make more “red” ?!

Dense & hyperaccreting disk can neutronize μ_e >~ $\theta = kT/m_e c^2$ [e.g. Beloborodov (2003)]

→ second timescales e.g. [Kiuchi+ (2023), Sprouse+ (2023)]

Neutrino-driven winds

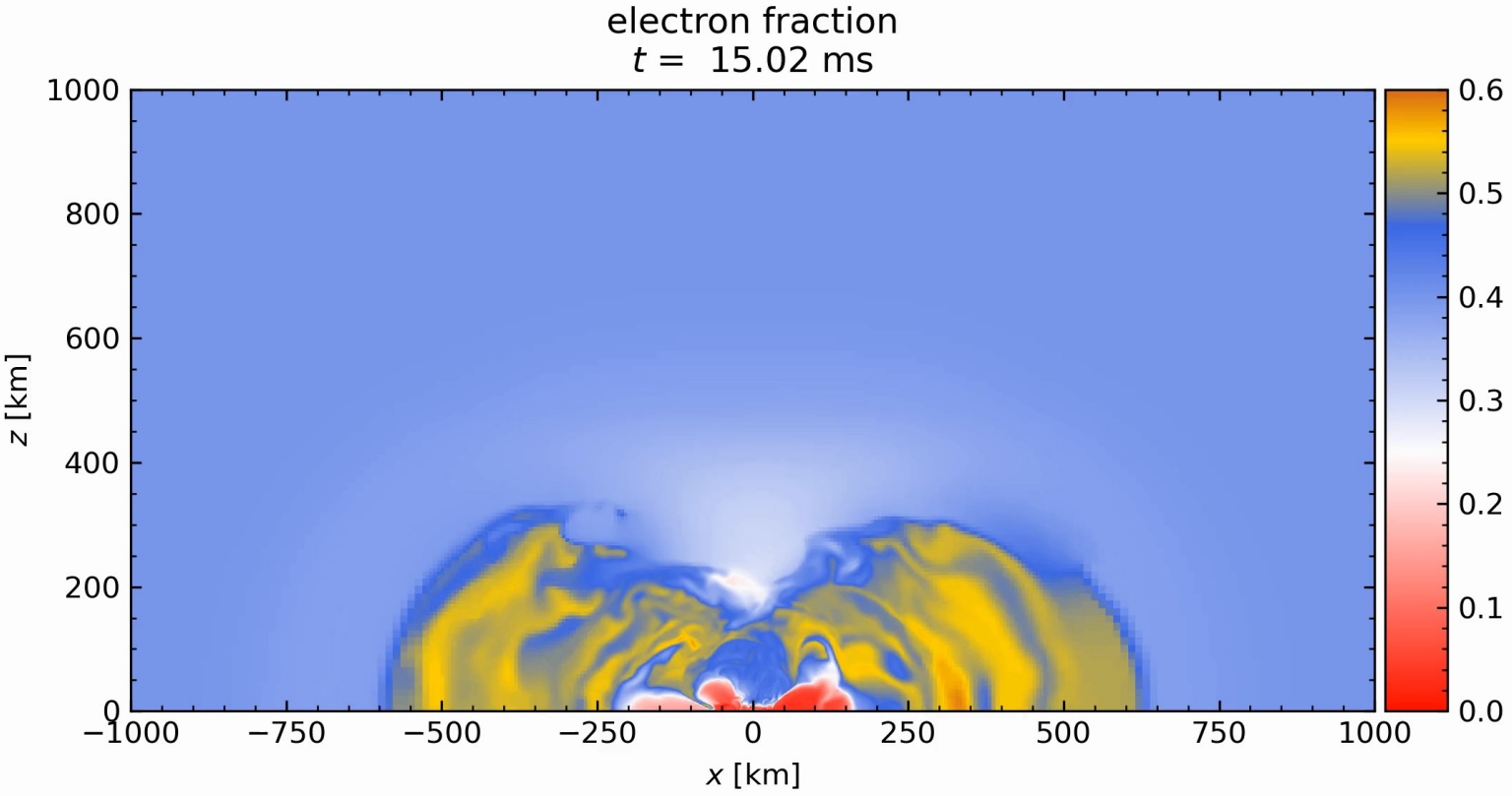

3D simulation to neutrino cooling timescale and collapse (~100ms postmerger)
Neutrino transport (M1) and turbulence sub-grid model (based on Kiuchi+ MHD data)

SB+ (2024)

Ejecta evolution with in situ nuclear network

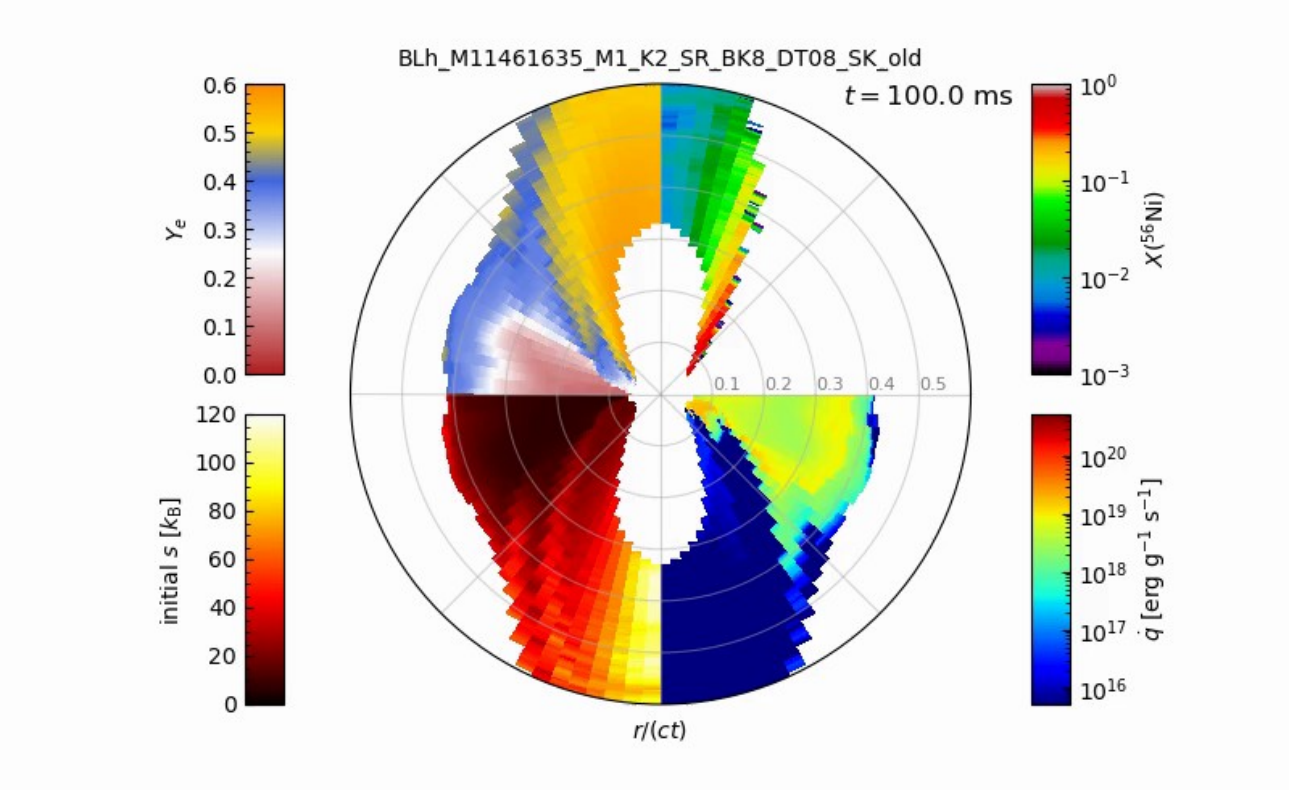

Jacobi, Magistrelli, SB+ (2025)

2D ray-by-ray radiation-hydro simulation with in situ nuclear network to ~ weeks timescales
knecNN (Magistrelli+ 2024) = SNEC (Morozova+ 2015) + SkyNet (Lippuner&Roberts 2017)

Ejecta evolution with in situ nuclear network

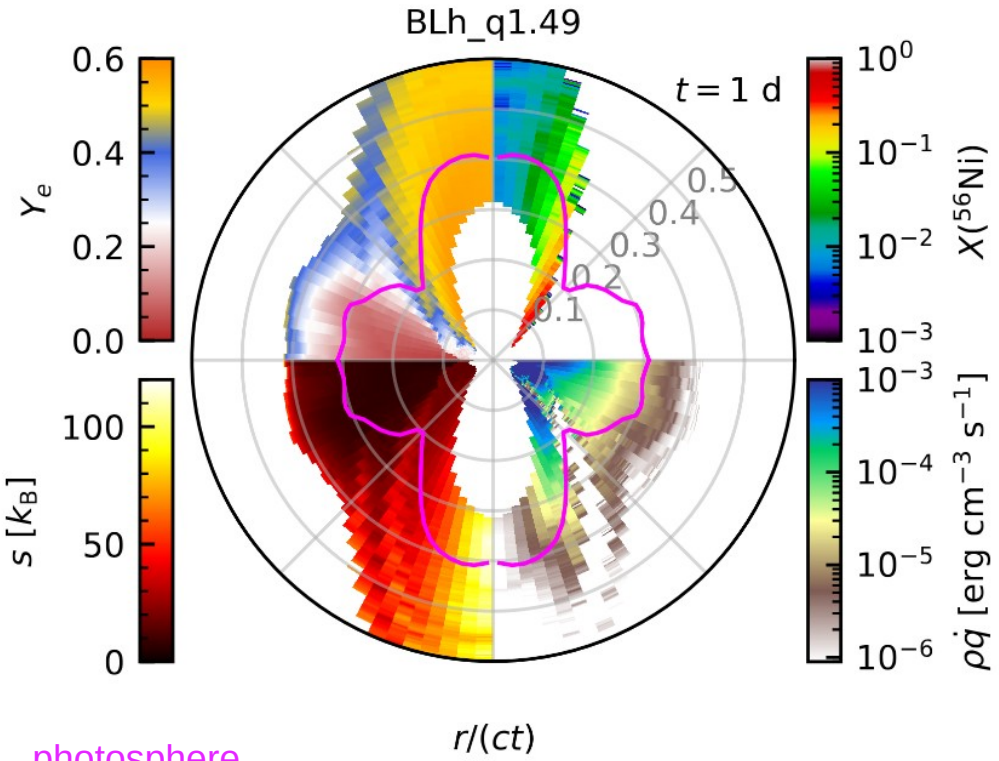

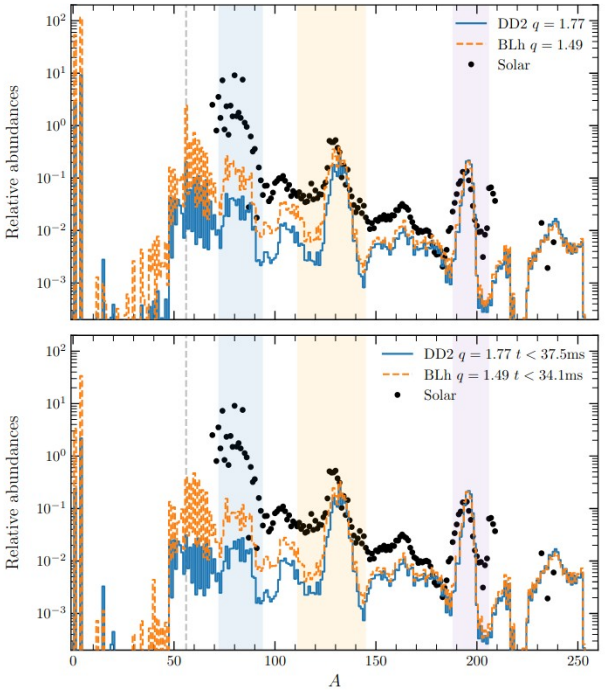

photosphere

SB+ (2024)

2D ray-by-ray radiation-hydro simulation with in situ nuclear network to ~ weeks timescales
knecNN (Magistrelli+ 2024) = SNEC (Morozova+ 2015) + SkyNet (Lippuner&Roberts 2017)

Not so heavy elements: 56Ni production

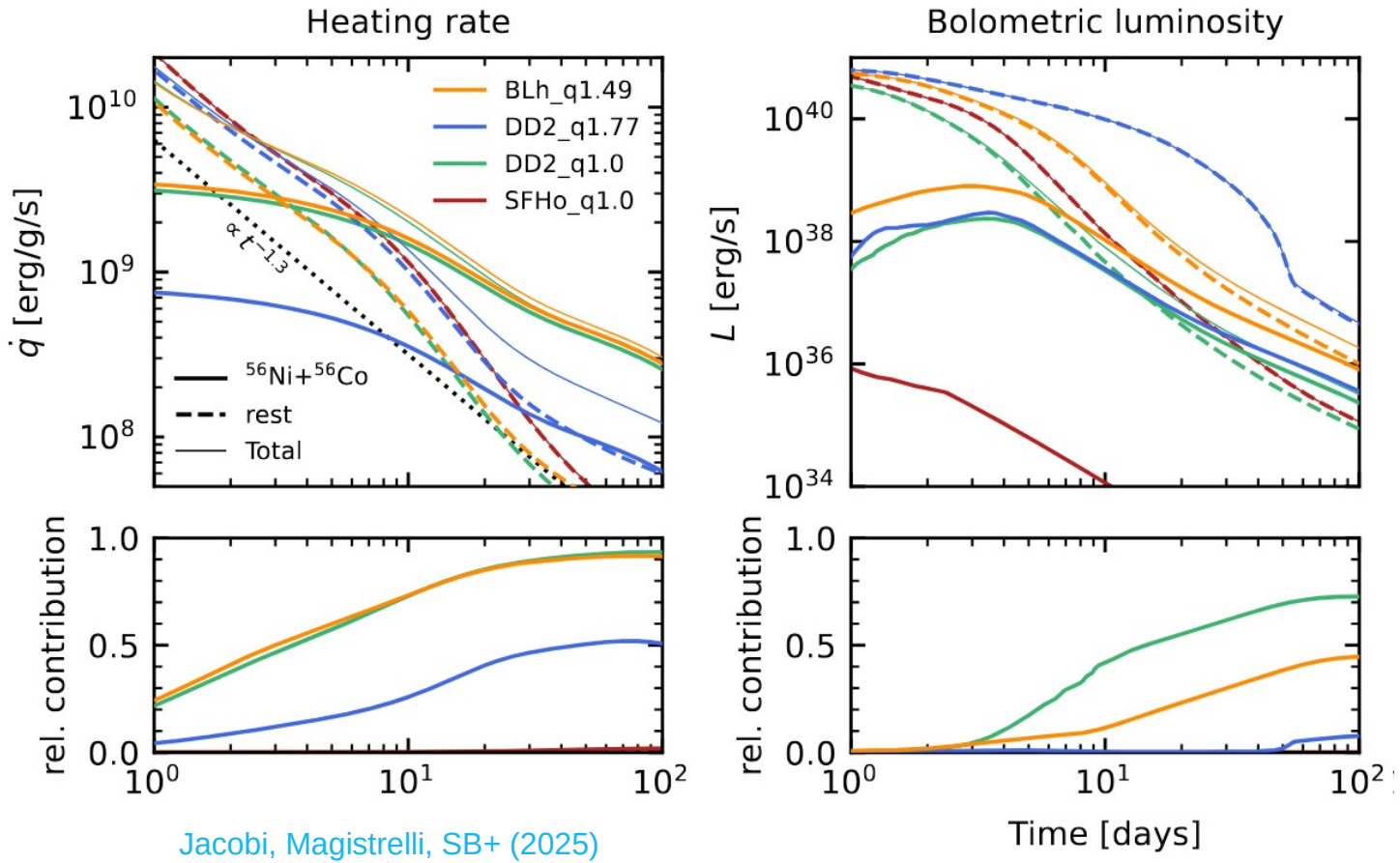

Jacobi, Magistrelli, SB+ (2025)

Not so heavy elements: 56Ni production

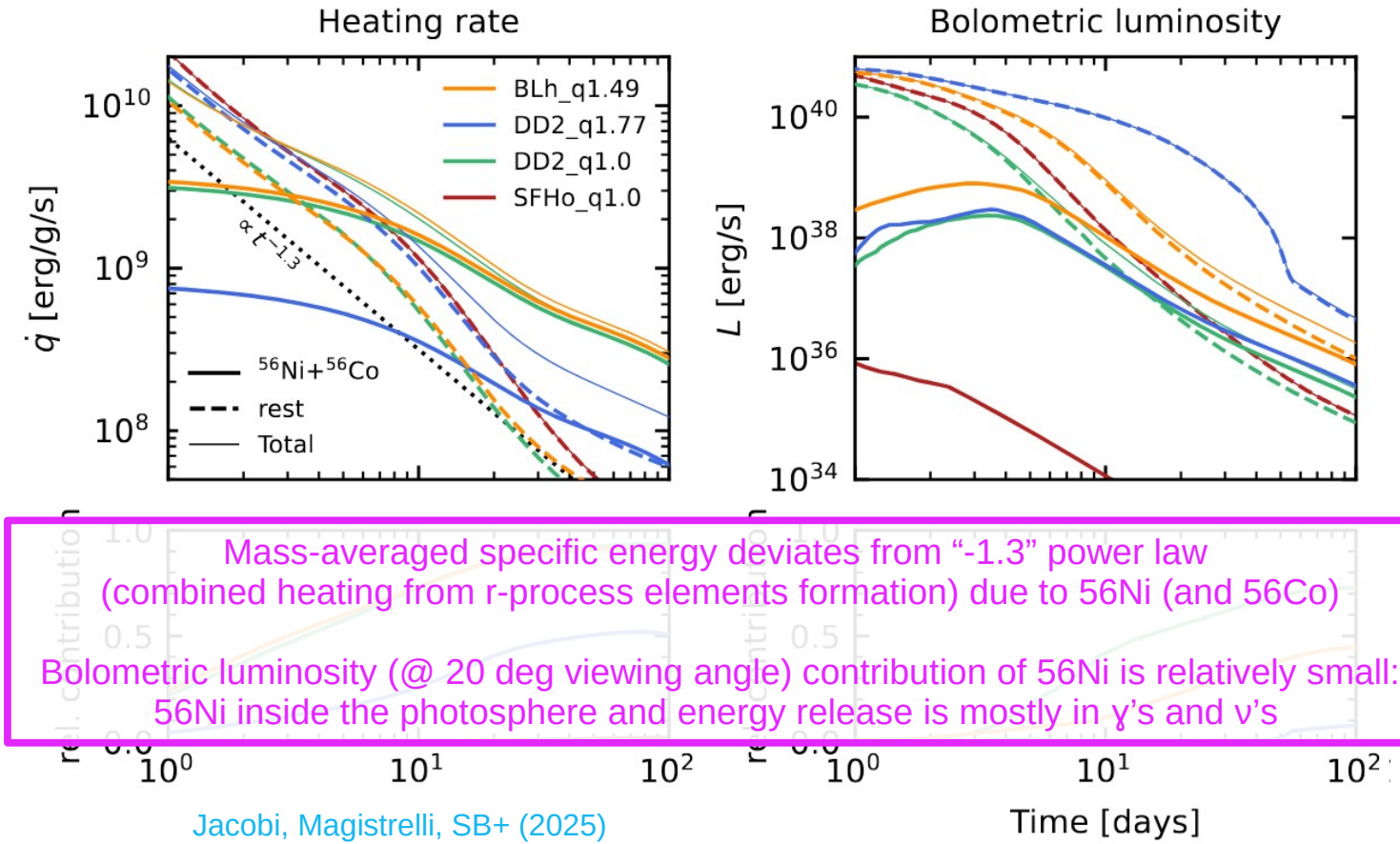

Mass-averaged specific energy deviates from “-1.3” power law
(combined heating from r-process elements formation) due to 56Ni (and 56Co)

Bolometric luminosity (@ 20 deg viewing angle) contribution of 56Ni is relatively small:
56Ni inside the photosphere and energy release is mostly in ɣ’s and ν’s

Jacobi, Magistrelli, SB+ (2025)

Not so heavy elements: 56Ni production

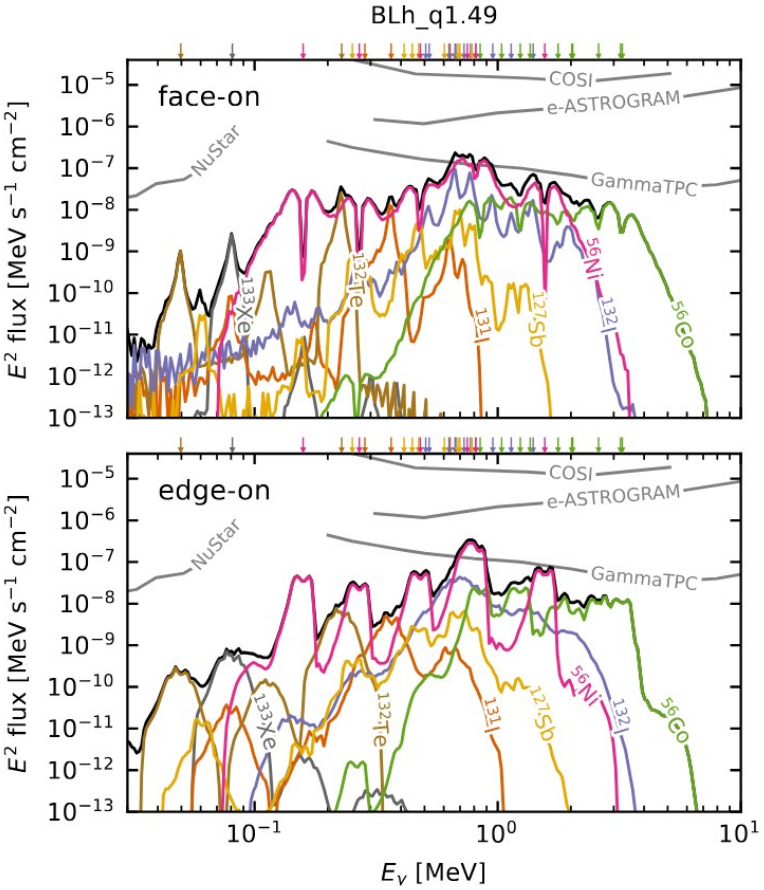

Jacobi, Magistrelli, SB+ (2025)

- ɣ emission from kN: 20-50% tot.rad.energy [Hotokenzaka+ (2016)]
- Light curves: large uncertainties in opacities and transport … but
  "*similar to thermonuclear SNe and CCSNe a more direct measurement of the yields can be obtained by observing the photons from the decay of radioactive nuclei in the ejecta*"
  [Korobkin+ (2020)]
- Here: include iron-group elements & Doppler shift
- Detectable 40Mpc with future instruments (700-800 KeV)
- Evidence for long-lived remnant (?)
- NB Presence of 56Ni unclear in AT2017gfo

Exascale numerical relativity

GR-Athena++ [Daszuta+ (2021),Cook+ (2023)] based on Athena++ (Stone+)

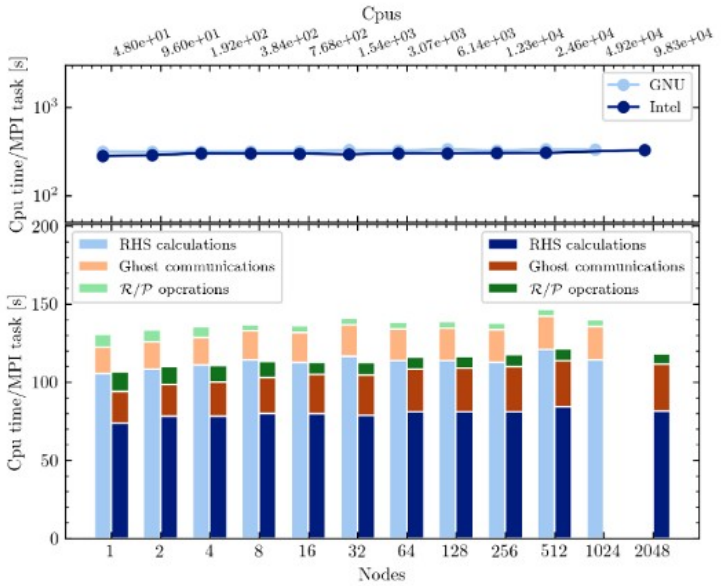

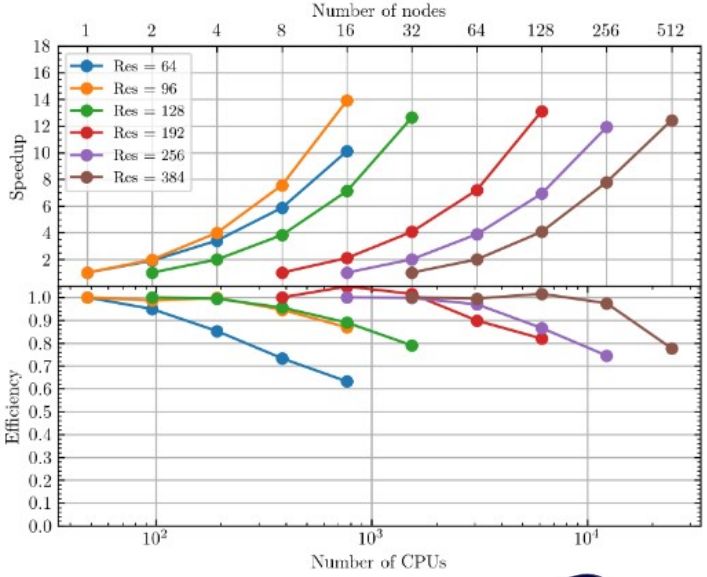

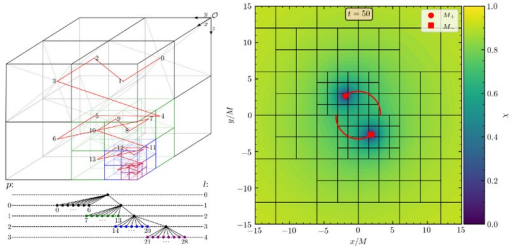

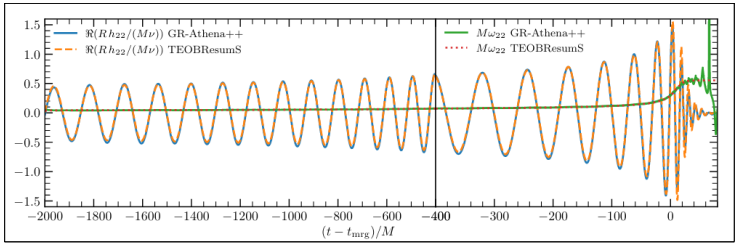

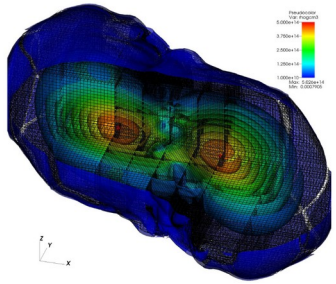

Exascale numerical relativity

GR-Athena++ [Daszuta+ (2021),Cook+ (2023)] based on Athena++ (Stone+)
(Performance-portable AthenaK [Stone+ (2024), Zhu+ (2024), Fields+ (2024)])

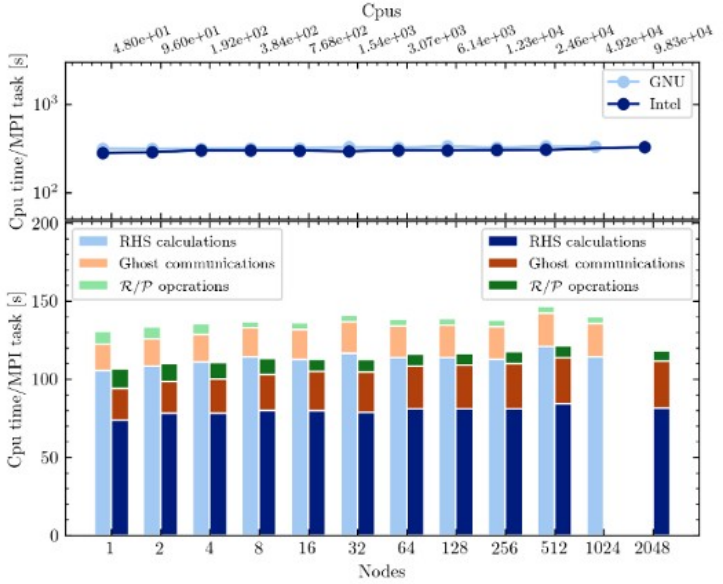

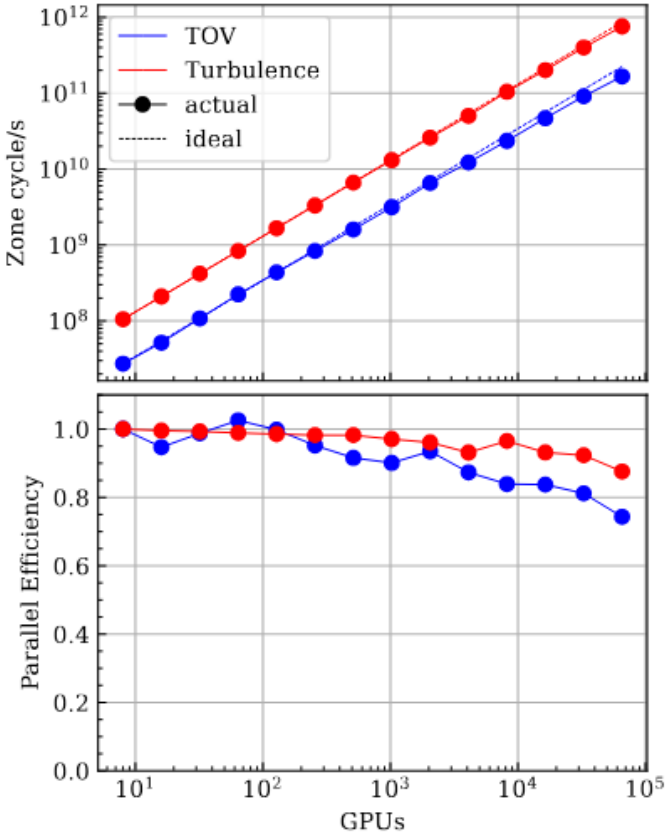

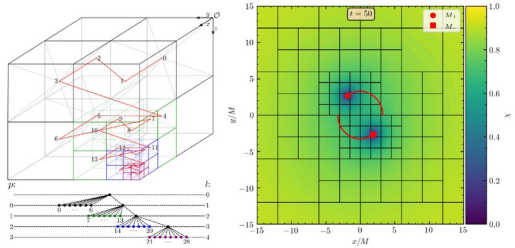

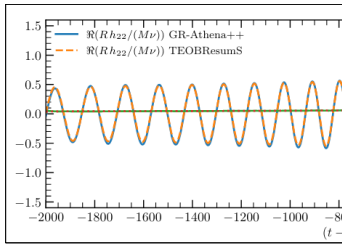

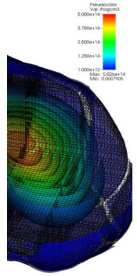

Conclusion

BNSMs are extreme astrophysical labs and rich sources of multi-messenger emissions. Theoretical modeling is essential for the interpretation of signals from BNSMs, viceversa BNSM are an ideal “playground" for a theorist (all fundamental interactions at the extreme!)

- Complete gravitational-wave models for BNSM are essential for signal detection and source inferences, e.g. to constrain NS matter via the measurement of tidal polarizability parameters and constraints on mass-radius diagram.
- Accurate & complete models start to be in place but systematics are not yet under control for high-precision measurements.
- Next-generation detectors will be senstitive to kHz GWs and could probe physical effects in extreme matter although unambiguous procedures for the detection of such effects are not yet available.

- Detailed (3+1)D multi-physics simulations of the merger aftermath are crucial for the interpretation of electromagnetic counterparts. State-of-art ab-inito simulations incorporate GR, MHD, microphysical EOS, and neutrino radiation.
- Kilonovae shine from multi-component & anisotropic mass ejecta; some properties correlate to the binary parameters → multi-messenger analyses.
- Simulations cannot yet quantitatively fit the observed AT2017gfo data, although many features are qualitatively explained.
- Nuclear and atomic uncertainties will be soon dominating predictions (?).

Backup slides

$$\partial_t \tilde{\Gamma}^i = -2\,\tilde{A}^{ij}\,\partial_j \alpha + 2\,\alpha \left[\tilde{\Gamma}^i{}_{jk}\,\tilde{A}^{jk} - \frac{3}{2}\,\tilde{A}^{ij}\,\partial_j \ln(\chi) \right.$$
$$\left. - \frac{1}{3}\,\tilde{\gamma}^{ij}\,\partial_j (2\,\hat{K} + \Theta) - 8\,\pi\,\tilde{\gamma}^{ij}\,S_j \right] + \tilde{\gamma}^{jk}\,\partial_j \partial_k \beta$$
$$+ \frac{1}{3}\,\tilde{\gamma}^{ij}\,\partial_j \partial_k \beta^k + \beta^j\,\partial_j \tilde{\Gamma}^i - (\tilde{\Gamma}_{\rm d})^j\,\partial_j \beta^i$$
$$+ \frac{2}{3}\,(\tilde{\Gamma}_{\rm d})^i\,\partial_j \beta^j - 2\,\alpha\,\kappa_1 \left[\tilde{\Gamma}^i - (\tilde{\Gamma}_{\rm d})^i \right],$$
$$\partial_t \Theta = \frac{1}{2}\,\alpha \left[R - \tilde{A}_{ij}\,\tilde{A}^{ij} + \frac{2}{3}\,(\hat{K} + 2\,\Theta)^2 \right]$$
$$- \alpha \left[8\,\pi\,\rho + \kappa_1\,(2 + \kappa_2)\,\Theta \right] + \beta^i \partial_i \Theta\,,$$

GR Formulation and Cauchy problem + GR hydrodynamics

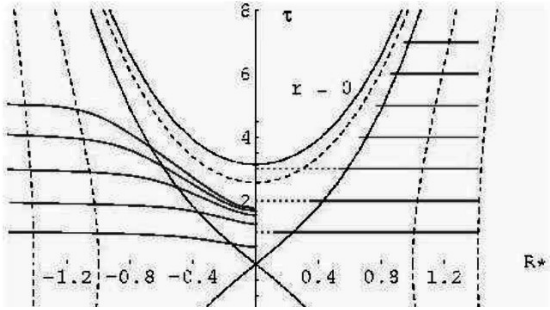

Coordinates and Singularities

Numerical relativity in a nutshell

Numerical methods for PDEs on adaptive grids

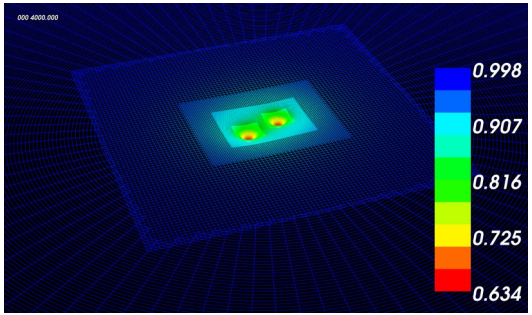

High-performance-computing (HPC)

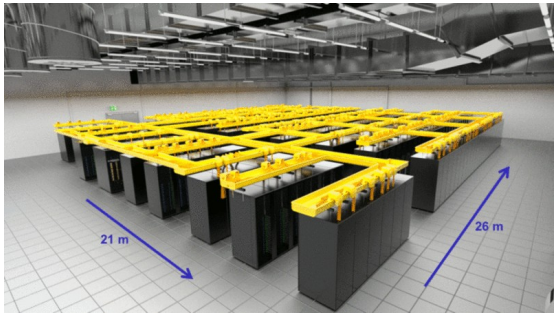

NATO ASI

CENTRE DE PHYSIQUE DES HOUCHES

M. T. Béal-Monod and D. Thoulouze Directors

2 June - 21 June 1982

RAYONNEMENT GRAVITATIONNEL

GRAVITATIONAL RADIATION

edited by

NATHALIE DERUELLE AND TSVI PIRAN

INSTITUT D'ÉTUDES AVANCÉES DE L'OTAN
NATO ADVANCED STUDY INSTITUTE

1983

NORTH-HOLLAND PUBLISHING COMPANY
AMSTERDAM · NEW YORK · OXFORD

GRAVITATIONAL RADIATION
AND
THE MOTION OF COMPACT BODIES

Thibaut Damour

Groupe d'Astrophysique Relativiste
Equipe de Recherche du C.N.R.S. n° 176
Observatoire de Paris-Meudon
92190 Meudon (France)

Using a post-Minkowskian approximation method supplemented by a technique of asymptotic matching, we obtain the general relativistic gravitational field outside two compact bodies (neutron stars or black holes). The equations of orbital motion of the compact bodies are deduced from the vacuum field equations by an Einstein-Infeld-Hoffmann-Kerr type approach simplified by the use of complex analytic continuation. The same process of analytic continuation allows one to push the accuracy of the calculations up to the third order: gravitational field containing cubic non-linearities and equations of motion deduced from the quartically non-linear vacuum Einstein equations. The equations of motion are explicitly written in Newtonian-like form as an expansion in powers of the inverse velocity of light up to the fifth order inclusively. The equations of motion up to c^{-4} are deduced from a generalized Lagrangian. The construction of Noetherian quantities conserved up to c^{-4} allows one to separate and investigate the c^{-5} secular kinematical effects caused by the finite velocity of propagation of gravity (Laplace-Eddington effect or "radiation damping"). These results agree with the phenomena observed in the Hulse-Taylor pulsar PSR 1913 + 16.

1. MOTIVATION

Two of the most remarkable features of Einstein's gravitational equations are:

1) their "hyperbolicity" (presence of propagation effects at a finite velocity),
2) their (infinite) non-linearity ("gravity generates gravity and influences its propagation").

It was soon realized (Einstein 1916) that the first feature implied the existence of wave-like solutions of the "linearized" vacuum field equations. Later these "linearized" waves were shown to be associated with an outgoing "energy flux" far from the system given, in the case of slow sources, by the famous "quadrupole formula" (Einstein 1918, see the lectures of K.S. Thorne and M. Walker in these proceedings):

3. DIGEST OF THE HISTORY OF THE PROBLEM OF MOTION

In 1687, I. Newton showed how the orbital motion of approximately spherical extended objects could be well-approximated by the motion of point masses. This is a very important result of Newtonian physics whose extension to General Relativity is highly non-trivial, as was pointed out by M. Brillouin (1922). M. Brillouin called this schematization of an extended body by a point mass with disappearance of all internal structure: "le principe d'effacement" ("effacing principle;" perhaps a more picturesque name would be: "the Cheshire cat principle"). In Newtonian physics the proof of this "effacing principle" makes an essential use of:

1) the linearity of the gravitational field as a function of the matter distribution (which allows one to define and separate the self-field and the external field);
2) the Action and Reaction principle (which allows one to define the center of mass and to ignore the contribution of the self-field to its motion);
3) Newton's theorem on the attraction of spherical bodies.

More specifically, for a binary system constituted of non-rotating nearly spherical bodies of masses m and m', one deduces from 1) that the main correction to the point mass idealization will come from the tidal field $Gm'd^{-3}r$ (where G is Newton's constant, r is the distance away from the center of mass of the first object m, and d is the distance between the two objects). If b denotes the radius of the first object, the tidal field will deform slightly its shape: $\delta b/b = h(m'/d^3)(b^3/m)$, where h, the first Love (1909) number, is a dimensionless quantity of order unity. This deformation induces in turn a small quadrupole moment: $Q = k\, m' b^5 d^{-3}$, where k, the second Love number, is a dimensionless quantity of order unity (h = 3/5 and k = 4/15 for the Earth). Finally this tidally induced quadrupole moment will create a small correction to Newton's law for point masses: $\delta F/F \sim k\,(b/d)^5$. Therefore as long as the radii of the objects are much smaller than their mutual distances, their internal structure (if they are not rotating) will be utterly negligible. We shall show in Section 5 how this result of "effacing" can be extended to Einstein's theory even, and in fact most accurately, in the case of compact objects, i.e. when the radius $b \sim Gm/c^2$. But as we shall not be able to use 1) and 2) above, we shall need a completely different approach to show that the very strong "self field" of the compact object does not contribute to its orbital motion.

Then one can find in vacuum a decoupled second order differential equation for $H = H_0 = H_2$ for instance (Edelstein and Vishveshwara 1970 , Demianski and Grishchuk 1974):

$$\hat{R}(\hat{R}-2)d^2(H/\hat{R}(\hat{R}-2))/d\hat{R}^2 + 3(2\hat{R}-2)d(H/\hat{R}(\hat{R}-2))/d\hat{R} - \\ - (L-2)(L+3)\, H/\hat{R}(\hat{R}-2) \quad = 0. \tag{10}$$

The general solution of this second order differential equation contains 2 arbitrary constants. For instance, when L = 2, one finds for the general quadrupolar H perturbation in vacuum, i.e. outside the body:

$$H = D(\hat{R}(\hat{R}-2) + k\,\hat{R}(\hat{R}-2)\int_{\hat{R}}^{\infty} 5dx/(x^3(x-2)^3)\,). \tag{11}$$

The dimensionless constant k is a relativistic generalization (Damour 1981) of the second Love number (Love 1909) which was introduced in Section 3. It is, in a sense, a dimensionless measure of the yielding of the object to an external tidal solicitation. It depends on the internal structure of the body (equations of state,...) and can be determined for an ordinary body (not a black hole) by imposing the regularity of the metric perturbation H, K, h_0 at the center of the body and when crossing the surface of the body (see e.g., Thorne and Campolattaro 1967). By our hypothesis 1) we have $\hat{R} \sim 1$ at the radius of the object, therefore as there are no other scales in the problem, k must be of order unity (like the non-relativistic one):

$$k \sim 1 \tag{12}$$

(More generally for non-necessarily compact objects of dimensionless radius $\hat{b}$, one will have $k \sim \hat{b}^5$ which allows one to justify the remark after hypothesis 1)). In the case of a black hole, k is determined by imposing the regularity of metric perturbation on the future horizon: in this case one finds k = 0 (in agreement with D'Eath 1975a). Incidently, one should not conclude from this result that there are no tidal responses of a black hole to an external solicitation: such a non-zero response is contained in the first term of the righthand side of (11): $\hat{R}\,(\hat{R}-2)$ which differs from the usual term (in absence of any object): $\hat{R}^2$.

PHYSICAL REVIEW D **85,** 123007 (2012)

Measurability of the tidal polarizability of neutron stars in late-inspiral gravitational-wave signals

Thibault Damour and Alessandro Nagar
Institut des Hautes Etudes Scientifiques, 91440 Bures-sur-Yvette, France ICRANet, 65122 Pescara, Italy

Loïc Villain
Laboratoire de Mathématiques et de Physique Théorique, Univ. F. Rabelais—CNRS (UMR 7350), Féd. Denis Poisson, 37200 Tours, France
(Received 20 March 2012; published 15 June 2012)

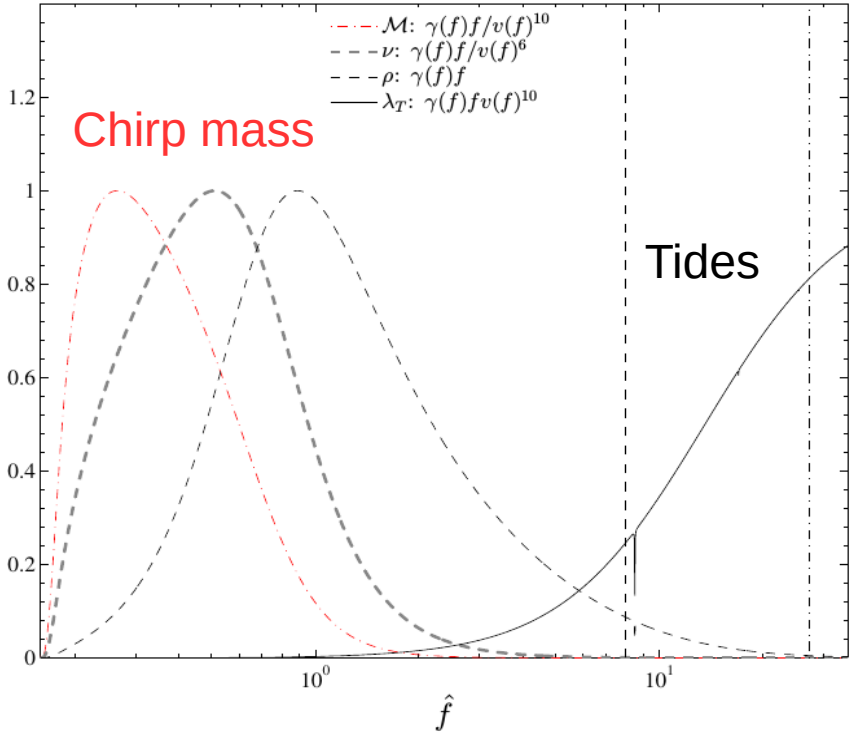

Post-merger detection with 3G are possible

Breschi,SB+ [https://arxiv.org/abs/2205.09112]

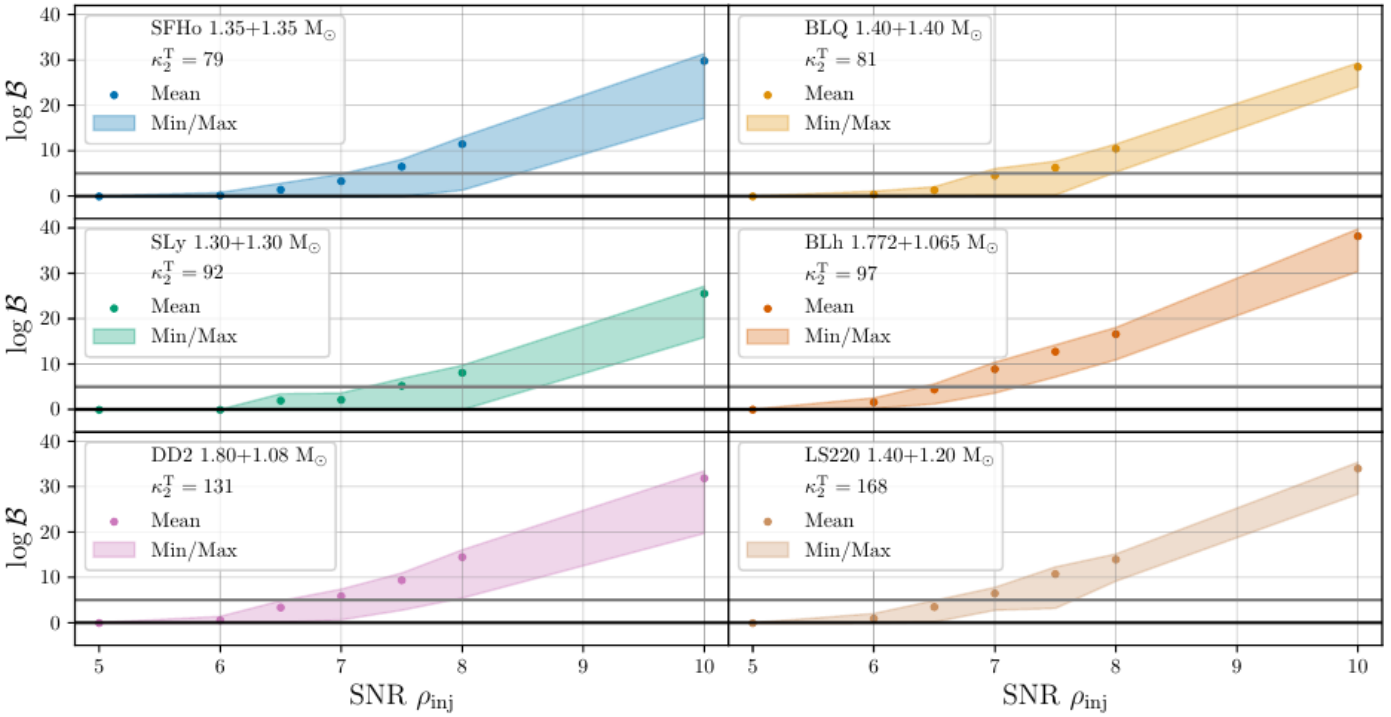

FIG. 5. Logarithmic BFs $\log \mathcal{B}$ as functions of the PM SNR $\rho_{\rm inj}$ of the injected NR template from Table I. The dots refer to the mean values averaged over the different noise realizations and the shadowed areas correspond to the minimum and maximum values recovered in the survey. Two horizontal lines identify $\log \mathcal{B} = 0$ (black) and $\log \mathcal{B} = 5$ (gray).

Weak interactions in the dynamical ejecta

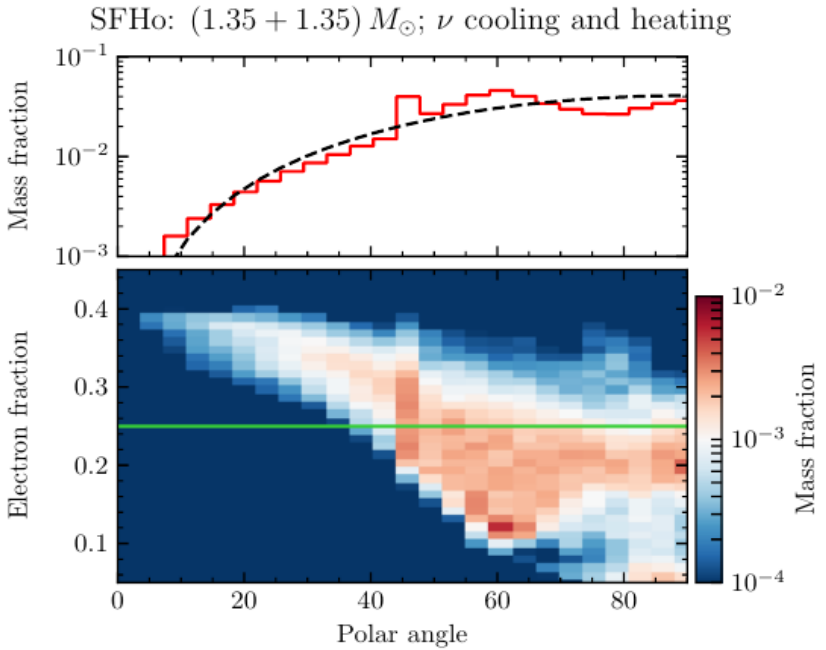

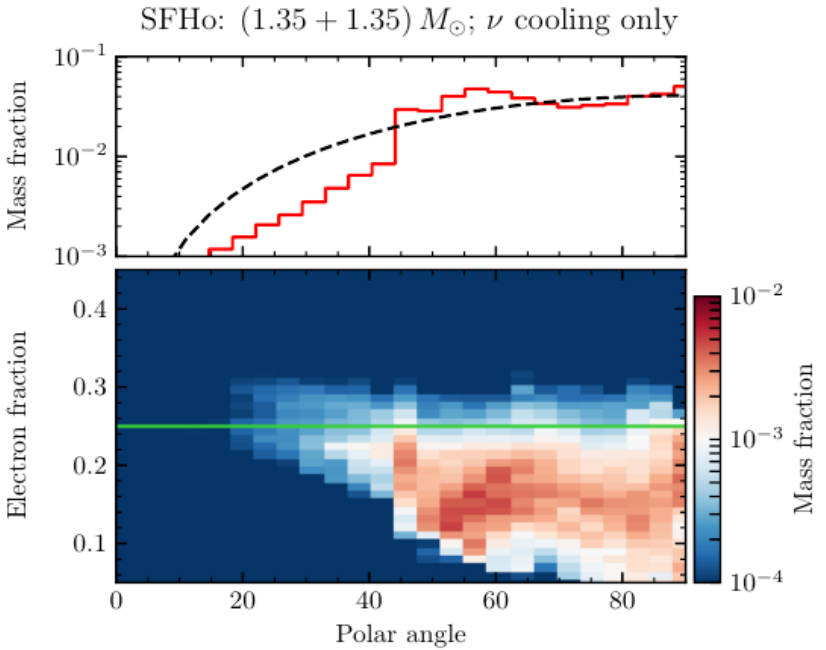

Neutrino absorption determines both composition and kinetic properties !

[Perego,Radice,SB ApJL 2017] See also [Wanajo+ 2014, Sekiguchi+ 2016, Foucart+ 2017/2018]

Discs around NS and BH remnants

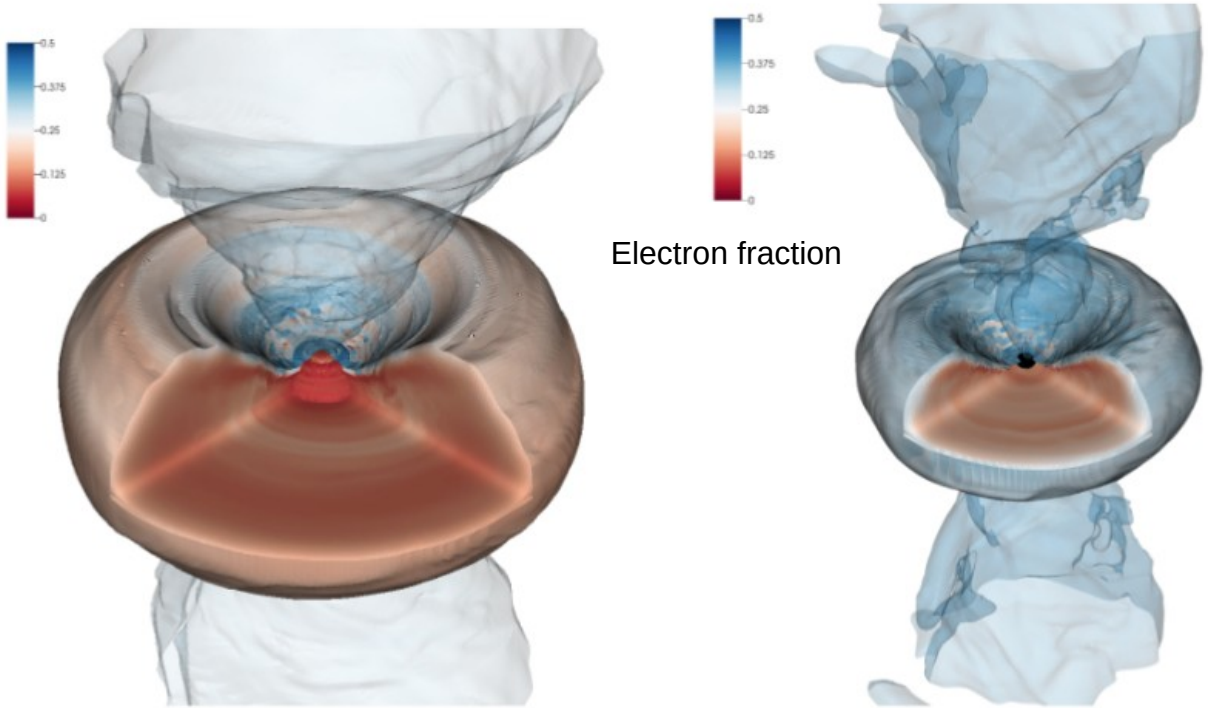

Perego, SB, Radice [https://arxiv.org/abs/1903.07898]

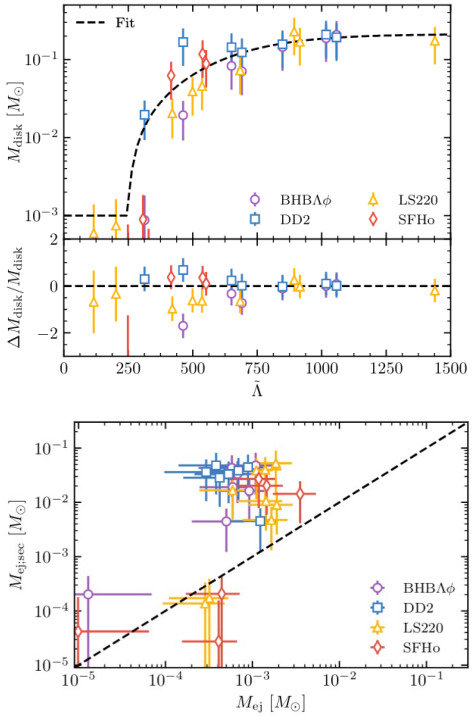

Figure 16. Dynamical ejecta $M_{\rm ej;dyn}$ versus secular ejecta masses $M_{\rm ej;sec}$. With the exception of the prompt BH formation cases that are able to expel at least a few $10^{-4}\,M_\odot$ in dynamical ejecta, the secular ejecta dominate over the dynamical ejecta.

Mass, compactness, composition depends on binary parameters and central remnant
Disc masses can be estimated from the reduced tidal parameter Λ (EOS-insensitive relation)
Disc winds significantly more massive than dynamical ejecta

[https://arxiv.org/abs/1809.11161]

Remnants after the GW-driven phase

- Angular momentum (“super-Keplerian”) and mass in excess
- Evolution governed by neutrino cooling and viscous processes (magnetic turbulence & stresses, neutrino heating, etc)
- Discs <~ 0.1Mo: Nuclear recombination → Massive winds

[Perego+ 2014]

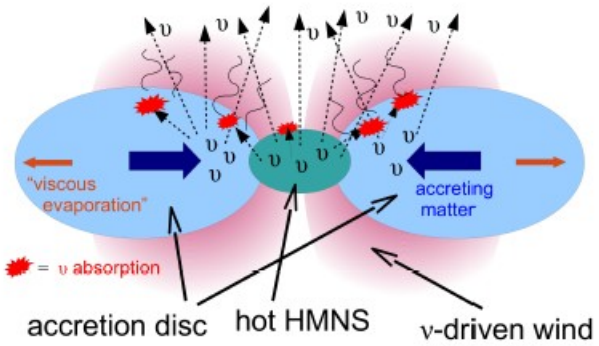

[Siegel+ 2014]

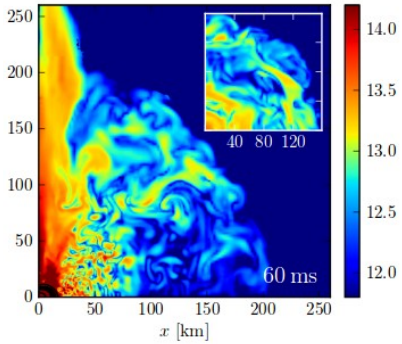

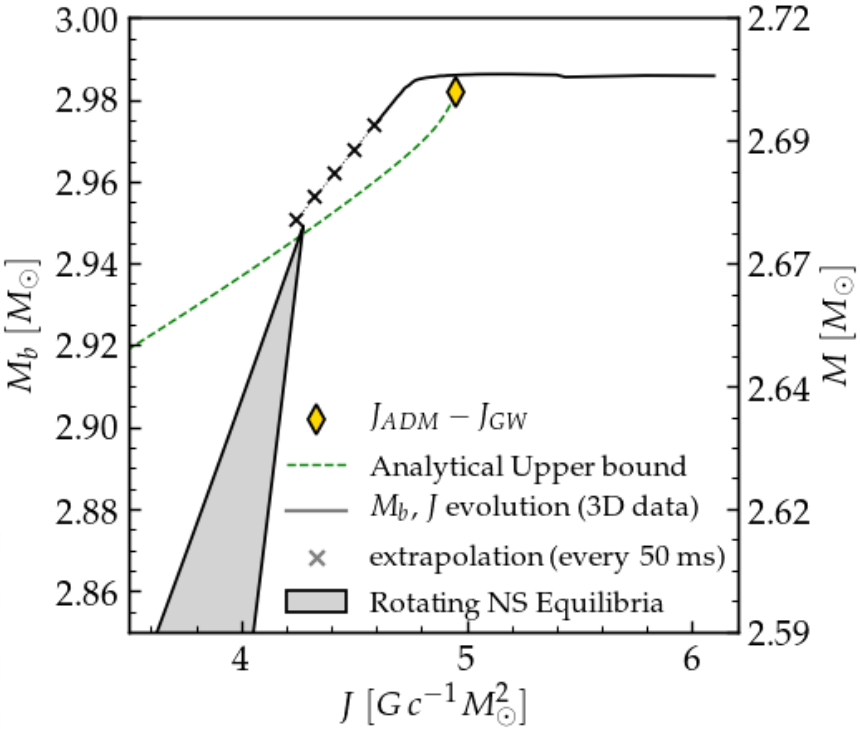

Radice, Perego, SB, Zhang [https://arxiv.org/abs/1803.10865]
Nedora, SB+ [https://arxiv.org/pdf/2008.04333]

Viscous phase

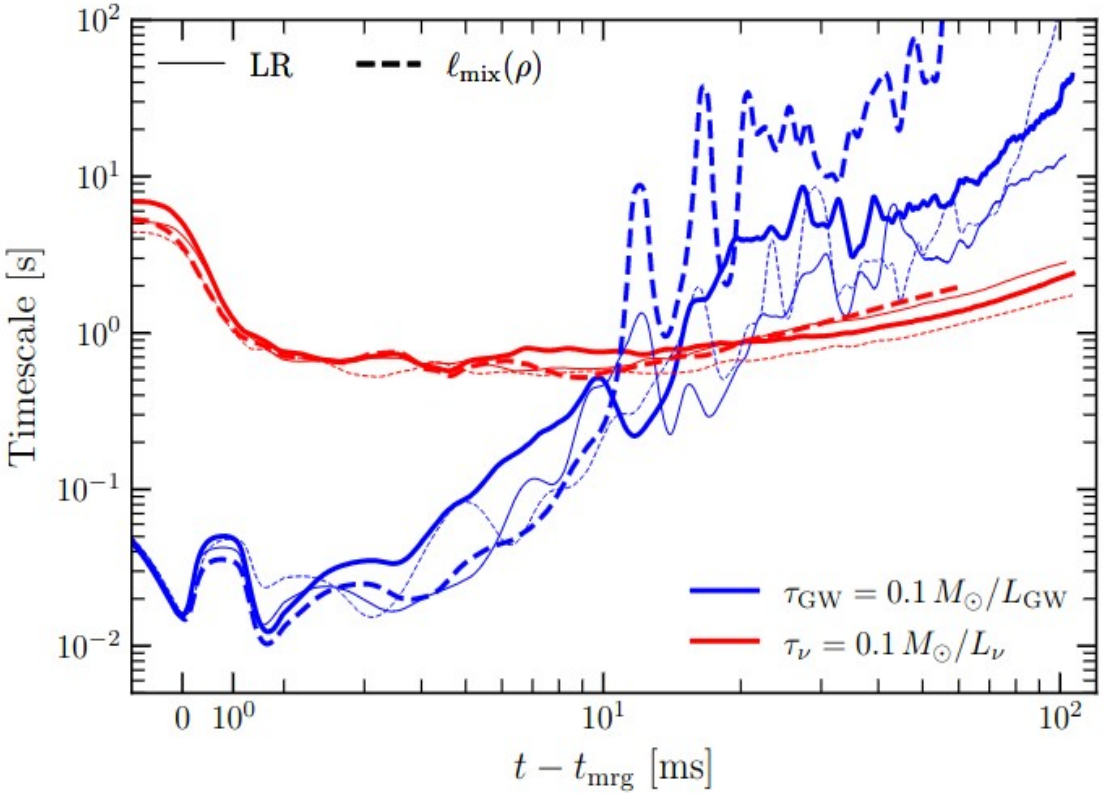

- NS remnant has angular momentum (“super-Keplerian”) and mass in excess
- Accretion discs: highly dependent on remnant (composition), non-Keplerian, hyperaccretion @ black hole formation, etc.
- Evolution governed by neutrino cooling and viscous processes (MHD turbulence & stresses, neutrino heating, etc)
- → quantitative predictions not yet available
- Indication for massive winds

Viscous phase: (3+1)D GR simulation w/ M1 and MHD subgrid model
Radice&SB [https://arxiv.org/abs/2306.13709]

Viscous phase

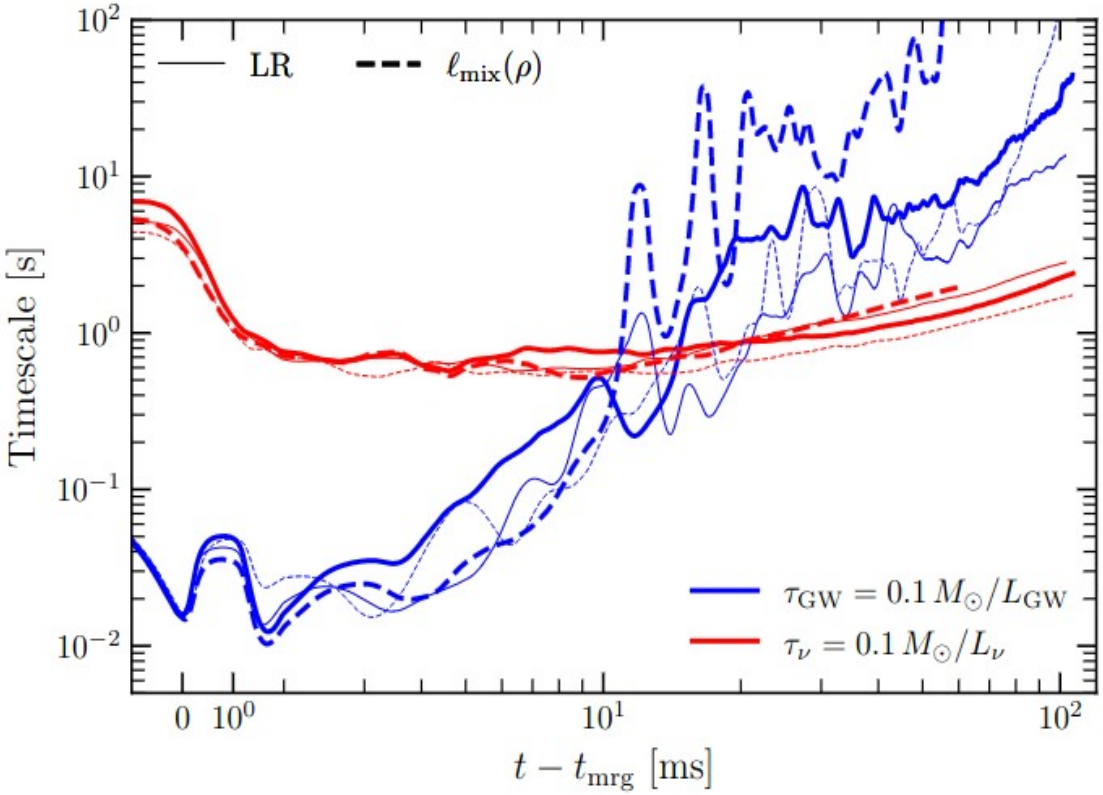

- NS remnant has angular momentum (“super-Keplerian”) and mass in excess
- Accretion discs: highly dependent on remnant (composition), non-Keplerian, hyperaccretion @ black hole formation, etc.
- Evolution governed by neutrino cooling and viscous processes (MHD turbulence & stresses, neutrino heating, etc)
- → quantitative predictions not yet available

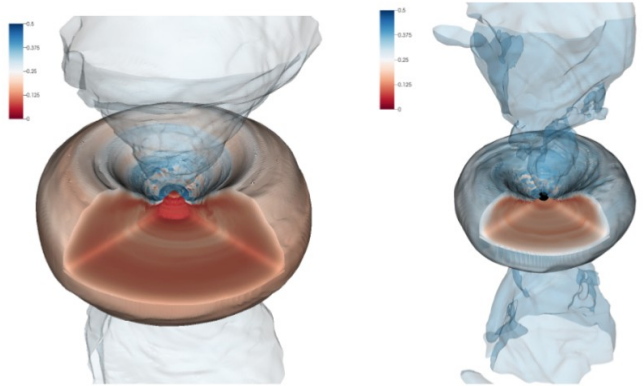

Viscous phase: (3+1)D GR simulation w/ M1 and MHD subgrid model
Radice&SB [https://arxiv.org/abs/2306.13709]

Perego, SB, Radice [https://arxiv.org/abs/1903.07898]

Long-lived Remnants: spiral-wave winds

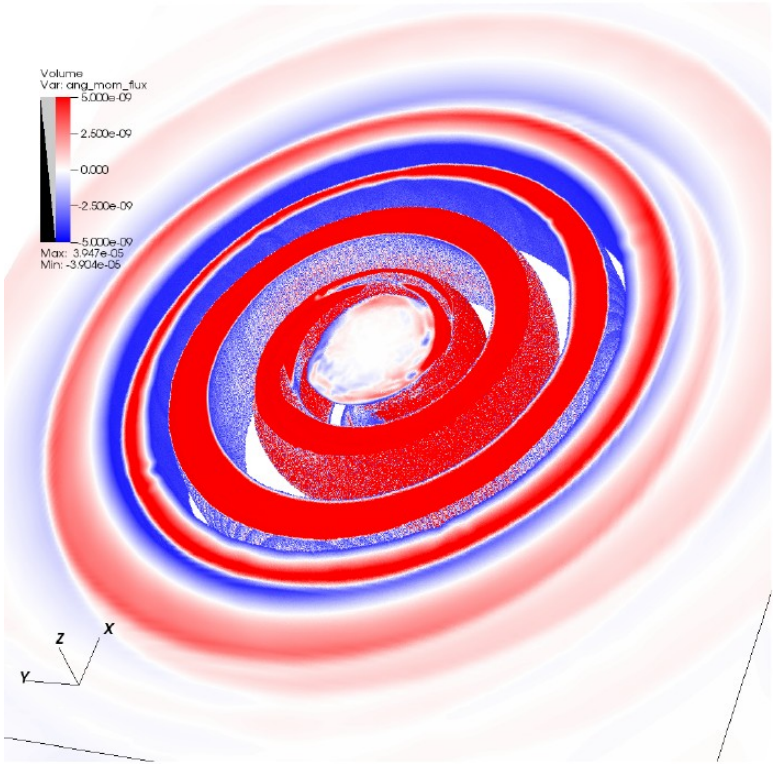

Nedora, SB+ [https://arxiv.org/abs/1907.04872]

Timescale ~ 10s ms postmerger (to collapse)
Mass ~ 0.01Mo (to 100ms)
Generic mechanism boosted by neutrino heating/MHD component

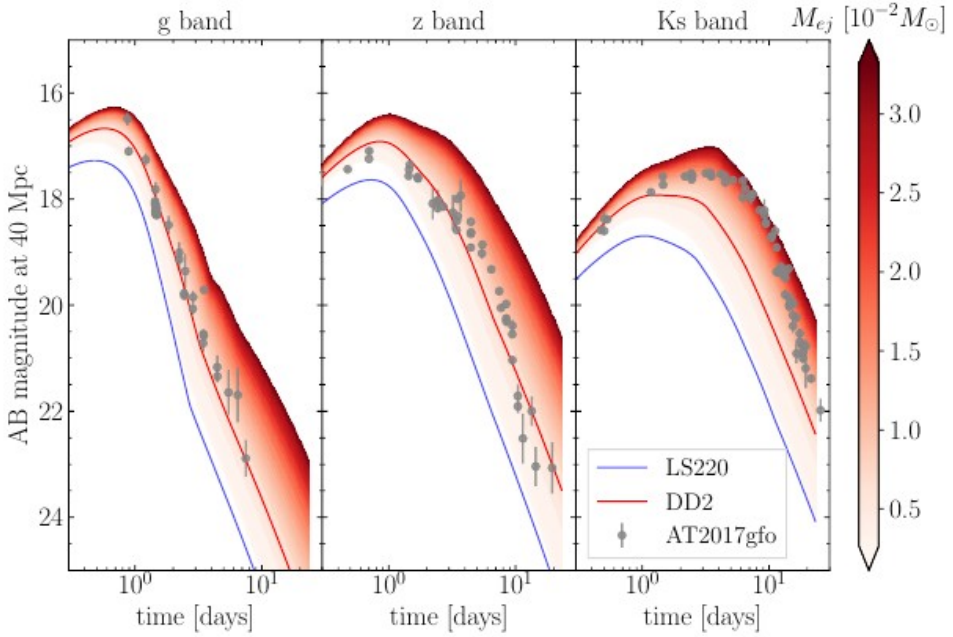

~100 ms 3D ab-inito evolutions with microphysics, M0 and GRLES (turbulent viscosity)

Kilonova basics

[Li&Paczynski 1998,Kulkani 2005,Metzger+ 2010,Kasen+ 2013,Grossmann+ 2014,Metzger LRR (2017)]

Kilonova: UV/optical/IR transient powered by the radioactive decay of freshly synthesized *r*-process elements

- high energy photons from nuclear decay
- photon thermalization in expanding ejecta
- thermal emission if:
  t_diffusion ~ t_expansion
- key parameters: ejecta velocity (v), opacity (k), and mass (m)

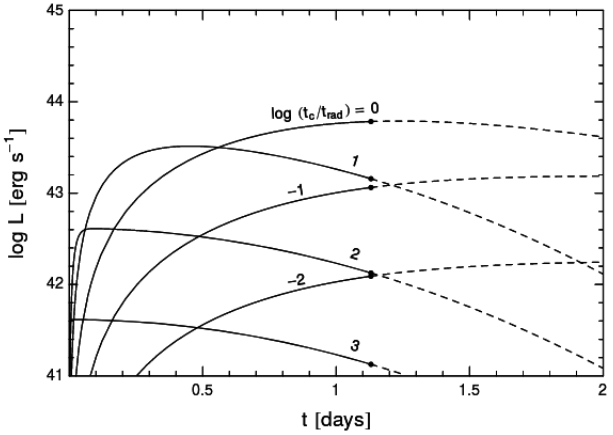

$$t_p \sim 4.9\,\mathrm{day}\left(\frac{\kappa}{10\,\mathrm{cm^2 g^{-1}}}\right)^{1/2}\left(\frac{m_{\rm ej}}{0.01\,M_\odot}\right)^{1/2}\left(\frac{v}{0.1c}\right)^{-1/2}$$

$$L_p \sim 2.5\times10^{40}\,\mathrm{erg\,s^{-1}}\left(\frac{\kappa}{10\,\mathrm{cm^2 g^{-1}}}\right)^{-\alpha/2}\left(\frac{m_{\rm ej}}{0.01\,M_\odot}\right)^{1-\alpha/2}\left(\frac{v}{0.1c}\right)^{\alpha/2}$$

$$T_p \sim 2200\,\mathrm{K}\left(\frac{\kappa}{10\,\mathrm{cm^2 g^{-1}}}\right)^{-(\alpha+2)/8}\left(\frac{m_{\rm ej}}{0.01\,M_\odot}\right)^{-\alpha/8}\left(\frac{v}{0.1c}\right)^{(\alpha-2)/8}$$

$$Q_{\rm nucl} = Q_{\rm nucl,0}\left(\frac{t}{1\,\mathrm{s}}\right)^{-\alpha}$$

alpha = 1.3

[Grossmann+ 2014]

Role of neutrino heating in nucleosynthesis

Systematic study of remnant and ejecta properties: neutrino schemes and mesh resolutions
Zappa, SB, Radice, Perego [https://arxiv.org/abs/2210.11491]

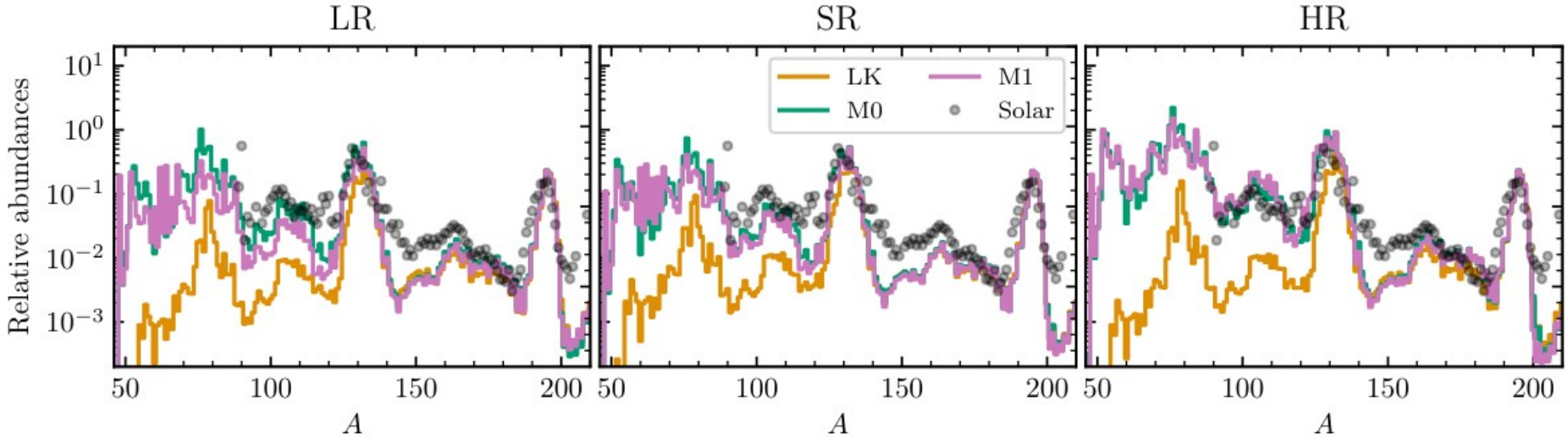

Gray M1 scheme with complete radiation-matter sources Radice,SB,Perego,Haas [https://arxiv.org/abs/2111.14858]

Impact of neutrino transport scheme

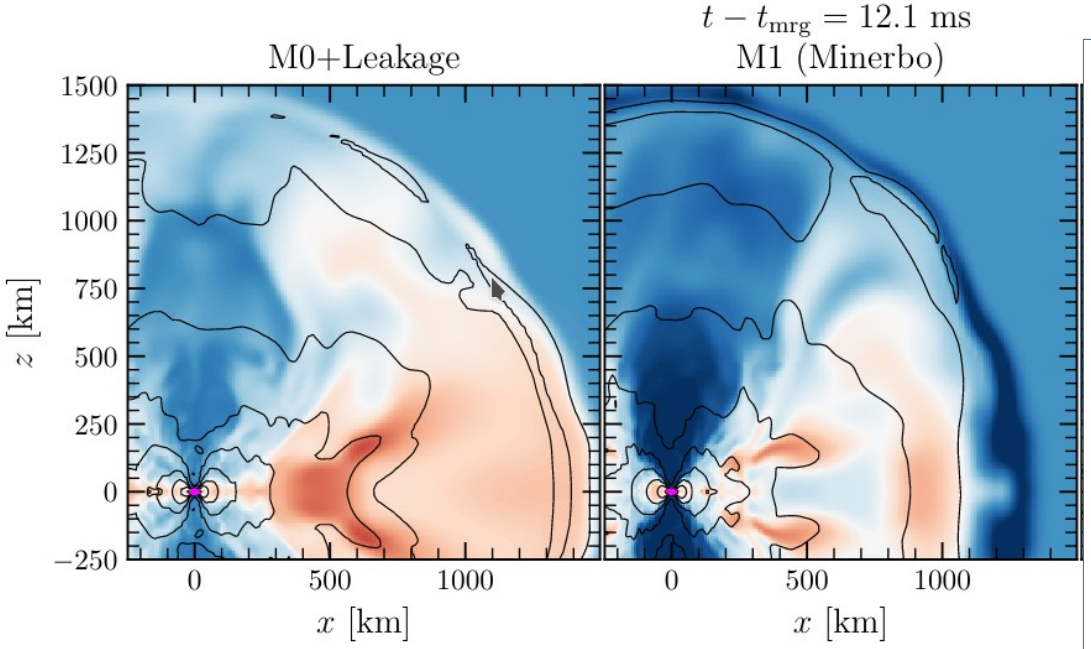

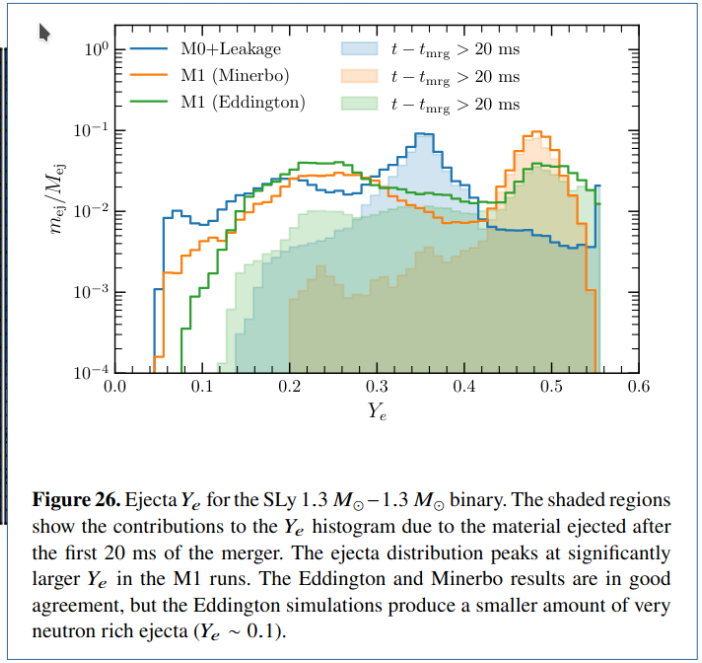

Figure 26. Ejecta Y_e for the SLy 1.3 $M_\odot$ – 1.3 $M_\odot$ binary. The shaded regions show the contributions to the Y_e histogram due to the material ejected after the first 20 ms of the merger. The ejecta distribution peaks at significantly larger Y_e in the M1 runs. The Eddington and Minerbo results are in good agreement, but the Eddington simulations produce a smaller amount of very neutron rich ejecta ($Y_e \sim 0.1$).

Figure 18. Electron fraction (color) of the dynamical ejecta cloud formed for the SLy 1.3 $M_\odot$ – 1.3 $M_\odot$ binary. The black lines are isodensity contours of $\rho = 10^5, 10^6, 10^7, 10^8, 10^9, 10^{10}, 10^{11}$, and 10^{12} g cm^{-3}. The purple contour shows corresponds to $\rho = 10^{13}$ g cm^{-3} and denotes the approximate location of the surface of the merger remnant. M0 and M1 results are in good qualitative agreement, but M1 predicts higher electron fractions for both the polar and equatorial ejecta.

Radice,SB,Perego,Haas [https://arxiv.org/abs/2111.14858]

AT2017gfo Bayesian inference

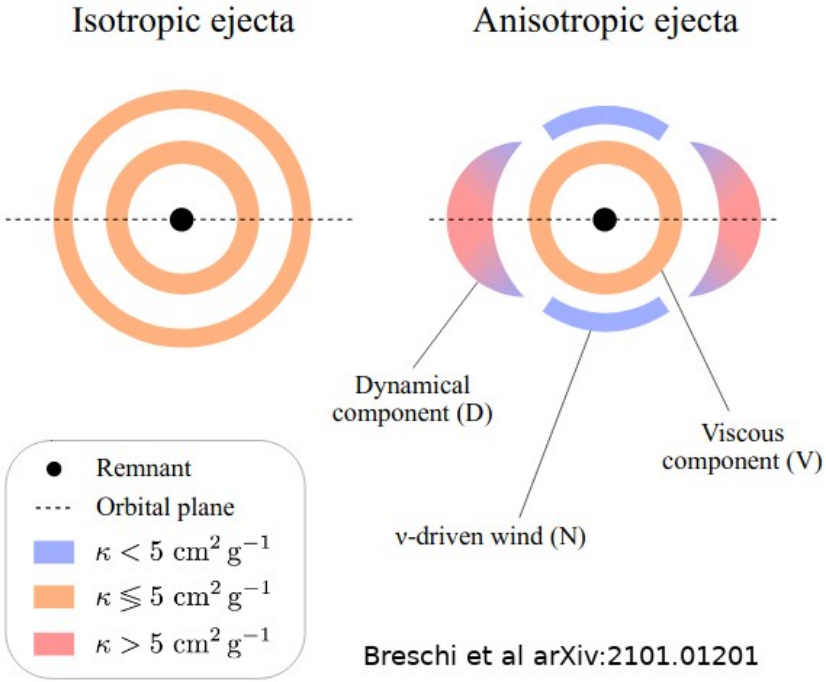

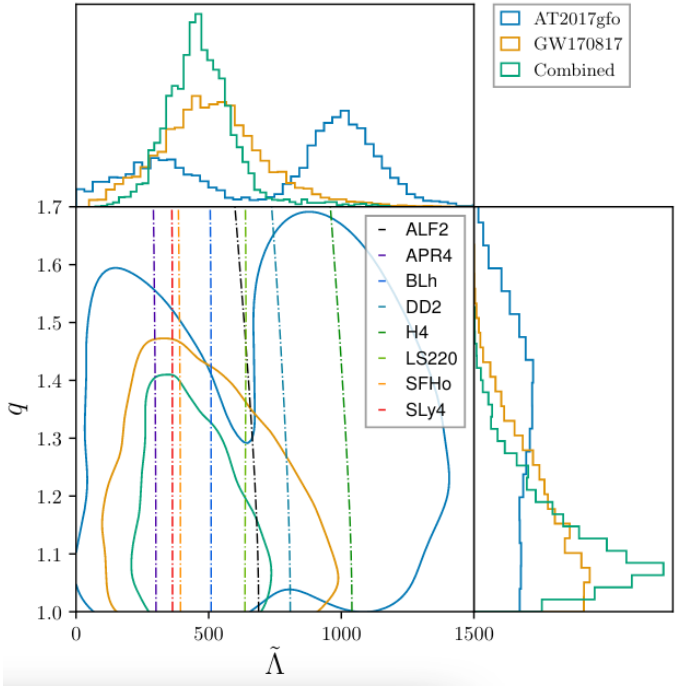

Bayesian model selection: 3-components + anisotropic models preferred
Breschi+ [https://arxiv.org/abs/2101.01201]

AT2017gfo requires disk formation, and thus constrains the reduced tidal parameter

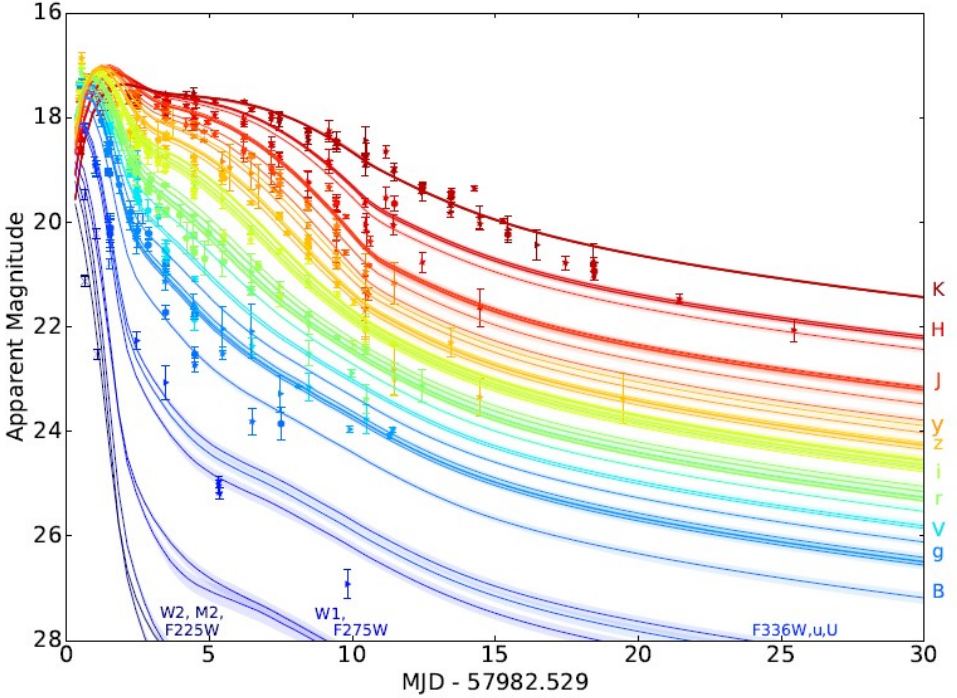

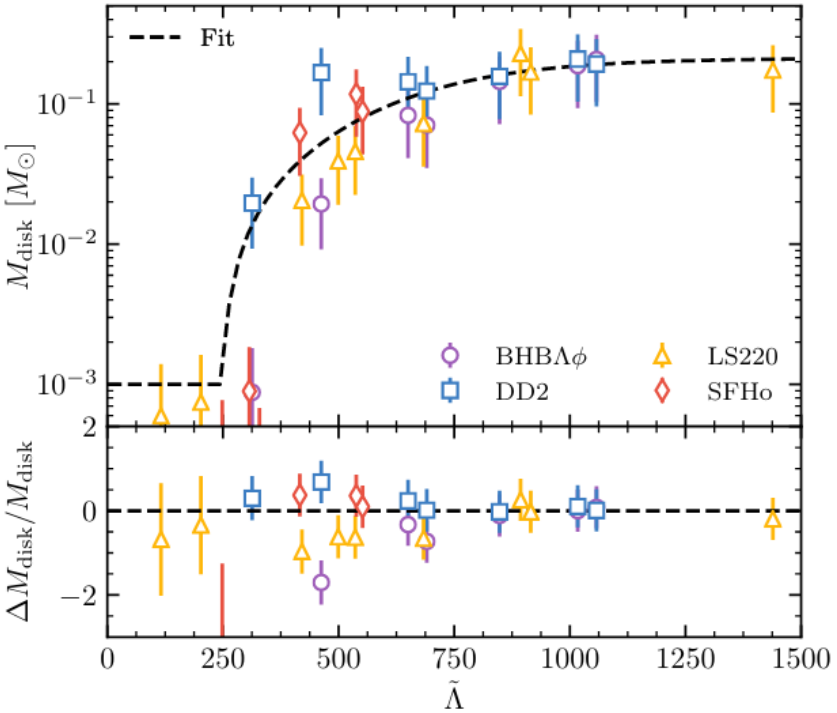

Radice,Perego,Zappa,SB [https://arxiv.org/abs/1711.03647]

Joint analyses to maximize science output

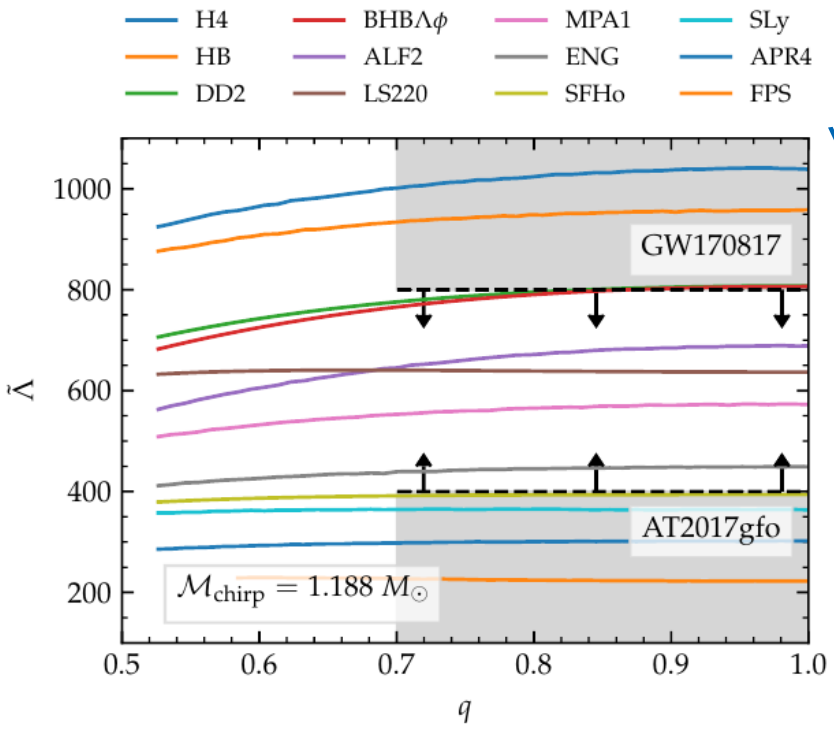

Waveform modeling

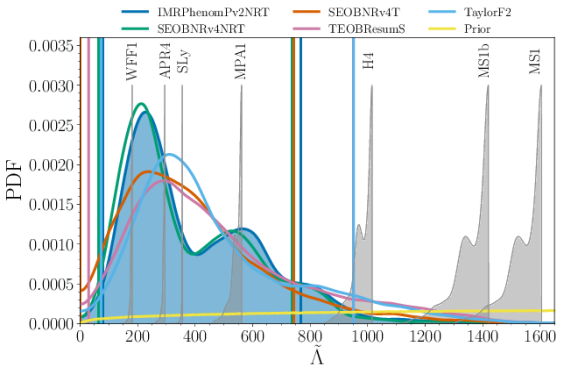

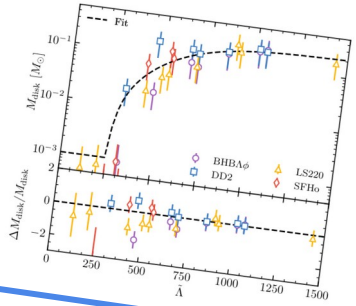

Remnant modeling

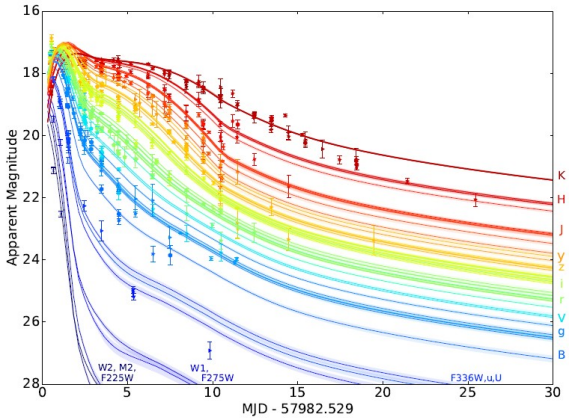

Radice,Perego,Zappa,SB [https://arxiv.org/abs/1711.03647] (proof-of-principle)
Breschi+ [https://arxiv.org/abs/2101.01201] (full Bayesian realization)